Twenty-Eighth Annual
Gaseous Electronics Conference
October 21-24, 1975

ROLLA, MISSOURI

28th GASEOUS ELECTRONICS CONFERENCE

PROGRAM

AND

ABSTRACTS

LOCAL ARRANGEMENTS COMMITTEE:

R.A. Anderson
R.J. Corbin
K.J. Nygaard
J.T. Park
W.R. Snow

A Topical Conference of
The American Physical Society

Sponsored by

University of Missouri - Rolla
American Physical Society
Division of Electron
And Atomic Physics

WITH THE ASSISTANCE OF:
THE OFFICE OF NAVAL RESEARCH

PROGRAM

TWENTY-EIGHTH ANNUAL

GASEOUS ELECTRONICS CONFERENCE

RECEPTION-MIXER AND REGISTRATION

8:00 PM - 10:00 PM
MONDAY, OCTOBER 20, 1975
THE BALLROOM - THE MANOR INN

SESSION AA. ARCS I - FLOW EFFECTS

8:30 AM - 10:00 AM, Tuesday, October 21
Ballroom West
Chairman: H.L. Witting, General Electric

AA-1 AXIAL SEPARATION OF CONSTITUENTS IN VERTICALLY BURNING ARCS (20 min.)
E. Fischer

AA-2+ SEGREGATION OF MINORITY SPECIES AND CONSTRICTION OF MERCURY ARCS CONTAINING SODIUM AND SCANDIUM IODIDES
R.J. Zollweg

AA-3+ DIFFUSION AND DEMIXING IN L.T.E. PLASMAS
R.W. Liebermann, G.L. Rogoff, and J. Vine

AA-4 PREDICTIONS OF EFFECTS OF NATURAL CONVECTION ON VERTICAL ARCS ENCLOSED IN A TUBE (7 min.)
J.J. Lowke

AA-5 DYNAMIC TEMPERATURE MEASUREMENTS IN RAMPED ARCS (7 min.)
D.M. Benenson and K-J Yang

AA-6 DISTRIBUTION OF ELECTRIC AND MAGNETIC QUANTITIES IN A MOVING ARC (7 min.)
D. Bhattacharyya, R. Bolton, and M. Drouet

+Combined presentation, total time alloted for both papers - 20 min.

SESSION AB. LASERS I: ENERGY DEPOSITION IN HIGH PRESSURE GASES
8:30 AM - 10:00 AM Tuesday, October 21
Ballroom East
Chairman: R.M. Hill, Stanford Research Institute

AB-1 TRANSIENT VIBRATIONAL POPULATIONS IN EXCITED STATES OF N_2 UNDER PULSED DISCHARGE CONDITIONS (7 min.)
D.C. Cartwright and N.A. Fiamengo

AB-2 ENERGY DISTRIBUTIONS OF ELECTRONS IN ELECTRON BEAM PRODUCED NITROGEN PLASMAS (7 min.)
D.R. Suhre and J.T. Verdeyen

AB-3 ELECTRON BEAM INITIATED He-Xe GAS DISCHARGE LASER (7 min.)
L.A. Newman and T.A. DeTemple

AB-4 ELECTRON-BEAM EXCITATION OF RARE-GAS-HYDROGEN MIXTURES (7 min.)
James K. Rice

AB-5 FLUORESCENCE EMISSIONS FROM MIXTURES OF MERCURY AND XENON (7 min.)
Joseph R. Woodworth

AB-6 ELECTRON ENERGY DISTRIBUTIONS IN AN E-BEAM INITIATED XENON PLASMA (7 min.)
A.E. Greene and C.J. Elliott

AB-7 A MONTE CARLO STUDY OF E-BEAM SCATTERING THROUGH FOILS AND GASES (7 min.)
Frank T. Wu, and Eric A. Lundstrom

AB-8 MODELLING OF HIGH PRESSURE ARGON-CESIUM DISCHARGES (7 min.)
N. Klein and B.E. Cherrington

SESSION BA. ARCS II: LTE AND ELECTRODES
10:30 AM - 12:00 Noon Tuesday, October 21
Ballroom West
Chairman: R.J. Zollweg, Westinghouse Research Labs

BA-1 ON LTE IN NITROGEN ARCS (7 min.)
J.P. Novak and J.P. Poulin

BA-2 THE TWO-DIMENSIONAL, CONSTANT PROPERTY ARC (7 min.)
I.M. Cohen and A.M. Whitman

BA-3 STUDIES OF THE ANODE REGION OF A HIGH INTENSITY ARGON ARC (7 min.)
J. Heberlein and E. Pfender

BA-4 STUDY OF THE ANCHORED CATHODE SPOTS OF A DC MERCURY VACUUM ARC (7 min.)
Gisela Eckhardt

BA-5 PLASMA INTERACTION WITH A ROUGH WALL (7 min.)
G.H. Ecker

SESSION BB. LASERS II: NOVEL LASER SCHEMES

10:30 AM - 12:00 Noon Tuesday, October 21
Ballroom East
Chairman: J. Jacob, Avco Everett

BB-1 DIRECT NUCLEAR PUMPED LASERS (20 min.)
G.H. Miley, J.T. Verdeyen, and W.E. Wells

BB-2 LASER ENHANCED COLLISIONAL ENERGY TRANSFER (7 min.)
M.G. Payne and M.H. Nayfeh

BB-3 POPULATION IVERSIONS IN HYDROGEN PLASMA NOZZLE FLOWS (7 min.)
W.L. Bohn

BB-4 INFLUENCE OF THE ELECTRON DENSITY ON THE MODES OF A PULSED SUBMILLIMETRE LASER (7 min.)
A. Hamonic and M.C. Sexton

BB-5 A VERY LOW DIVERGENCE N_2 UV LASER (7 min.)
Bruno Godard

BB-6 ENERGY PATHWAYS FOLLOWING PROTON EXCITATION OF Ar-N_2-SF_6 GAS MIXTURES (7 min.)
C.H. Chen, J.P. Judish, G.S. Hurst, and M.B. Payne

SESSION C. ELECTRON COLLISIONS I: ELECTRON SCATTERING, EXCITATION, AND IONIZATION

1:30 PM - 3:15 PM, Tuesday, October 21
Ballroom East
Chairman: A. Phelps, Joint Institute for Laboratory Astrophysics

C-1 MOMENTUM TRANSFER CROSS SECTION FOR ELECTRON-ARGON COLLISIONS (20 min.)
R.W. Crompton and H.B. Milloy

C-2 EXPERIMENTAL AND THEORETICAL INVESTIGATION OF DIFFUSION COOLING OF ELECTRONS IN H_2-Ar MIXTURES (7 min.)
R.W. Crompton, T. Rhymes, and R.E. Robson

C-3 ELASTIC SCATTERING OF ELECTRONS IN MOLECULAR HYDROGEN (7 min.)
B. Van Wingerden, F.J. De Heer, E. Weigold, and K.J. Nygaard

C-4 ELECTRON EXCITATION OF THE SODIUM ATOM (7 min.)
James O. Phelps and Chun C. Lin

C-5 ELECTRON IMPACT CROSS SECTION MEASUREMENT OF HELIUM ($2^3S \rightarrow 3^3P$) (7 min.)
M.L. Lake

C-6 EXCITATION OF THE 2A AND 3A STATES OF H_2 BY ELECTRON IMPACT (7 min.)
J. Watson, Jr., and R.J. Anderson

C-7 MEASUREMENTS OF THE ELECTRON IMPACT IONIZATION CROSS SECTIONS OF Rb^+ IONS (7 min.)
R.K. Feeney, W.E. Sayle II, and T.F. Divine

C-8 EXPERIMENTAL-THEORETICAL COMPARISONS OF $1^1S \rightarrow 3^1P_{\pm 1}$ DIFFERENTIAL MAGNETIC SUBLEVEL CROSS SECTIONS IN e-He SCATTERING (7 min.)
A. Chutjian

SESSION DA: ARCS III: RADIATION, EMISSION, AND DIAGNOSTICS

3:45 PM - 5:30 PM, Tuesday, October 21
Ballroom West
Chairman: D.M. Benenson, SUNY/Buffalo

DA-1 RADIATION EMISSION COEFFICIENTS FOR SULFUR HEXAFLUORIDE ARC PLASMAS (7 min.)
R.W. Liebermann and J.J. Lowke

DA-2 MOLECULAR AND EXCITED I CONTINUUM RADIATION FROM METAL IODIDE RCS (7 min.)
R.J. Zollweg and R.W. Liebermann

DA-3 AXIS ATOM DENSITY MEASUREMENTS IN METAL-HALIDE ARCS (7 min.)
M. Adriaansz and L. Vriens

DA-4 OPTICAL ABSORPTION OF TIN DI-HALIDE MOLECULES AS A FUNCTION OF TEMPERATURE (7 min.)
P.C. Drop and J.H. Verduin

DA-5 MEASUREMENTS OF Ly-α AND -β LINE PROFILES IN AN ARGON ARC (7 min.)
G.L. Weissler and Hans-H Carls

DA-6 TEMPERATURE MEASUREMENTS IN A FREE BURNING ARC (7 min.)
S.S. Glickstein

DA-7 NON-LTE SPECTROSCOPIC ANALYSIS OF A LOCAL FLUIDIZED CONSTRICTION OF A WALL STABILIZED ARGON ARC (7 min.)
T.L. Eddy, C.J. Cremers and H.S. Hsia

SESSION DB. ELECTRON COLLISIONS II: RECOMBINATION AND DISSOCIATION

3:45 PM - 5:30 PM, Tuesday, October 21
Ballroom East
Chairman: K.J. Nygaard, University of Missouri-Rolla

DB-1 THE HIGH PRESSURE HELIUM AFTERGLOW AT ROOM TEMPERATURE (7 min.)
R. Deloche, P. Monchicourt, M. Cheret, and F. Lambert

DB-2 THE IMPORTANCE OF RECOMBINATION OF MOLECULAR HELIUM IONS IN HELIUM AFTERGLOWS (7 min.)
C.P. de Vries and H.J. Oskam

DB-3 RATE COEFFICIENTS FOR EXCITATION OF $O_2(b^1\Sigma_g^+)$ BY ELECTRONS (7 min.)
S.A. Lawton and A.V. Phelps

DB-4 ELECTRON TEMPERATURE DEPENDENCE OF RECOMBINATION OF ELECTRONS WITH AMMONIUM SERIES IONS, $NH_4^+ \cdot (NH_3)_n$
Chou-Mou Huang, Manfred A. Biondi, and Rainer Johnsen

DB-5 DISSOCIATION OF THE OXYGEN MOLECULE BY ELECTRON COLLISION (7 min.)
Sunggi Chung and Chun C. Lin

DB-6 THE DISSOCIATIVE EXCITATION OF THE LYMAN AND BALMER SERIES OF HYDROGEN BY ELECTRON IMPACT ON CH_4 (7 min.)
R.W. McLaughlin and E.C. Zipf

DB-7 DISSOCIATIVE IONIZATION OF $C\ell_2$ and HCℓ BY ELECTRON IMPACT FROM THRESHOLD TO 100 eV (7 min.)
M.C. Marden and W.R. Snow

DB-8 KINETIC ENERGY AND ANGULAR DISTRIBUTIONS OF N^+ FROM DISSOCIATIVE IONIZATION OF N_2 (7 min.)
R.J. Van Brunt and L.J. Kieffer

DB-9 FAST METASTABLE FRAGMENTS PRODUCED BY DISSOCIATIVE EXCITATION OF CARBONYL SULFIDE (7 min.)
R.J. Van Brunt and M.J. Mumma

DB-10 THE DISSOCIATIVE EXCITATION OF H_2, HD, AND D_2 BY ELECTRON IMPACT (7 min.)
B.L. Carnahan and E.C. Zipf

SESSION E. WORKSHOP I: ARC-PLASMA PROCESSING

7:30 PM, Tuesday October 21
Manor Inn
Discussion Leader: E. Pfender, University of Minnesota

E-1 THE ROLE OF ARC GAS HEATERS IN AN ELECTRIC ECONOMY
M.G. Fey

E-2 REACTORS FOR PLASMA PROCESSING
W.H. Gauvin

E-3 PLASMA PROCESSING IN EXTRACTIVE METALLURGY
D.R. MacRae

E-4 ARC COAL PROCESS FOR CONVERTING COAL TO ACETYLENE
R.E. Gannon

SESSION F. HEAVY PARTICLE COLLISIONS I

8:30 AM - 10:30 AM, Wednesday, October 22
Ballroom East
Chairman: N. Lane, Rice University

F-1 ROTATIONALLY ELASTIC AND INELASTIC COLLISIONS OF ELECTRONS WITH POLAR MOLECULES (25 min.)
F.T. Smith, D.L. Huestis, D. Mukherjee, and W.H. Miller

F-2 A NEW MULTISTATE SEMICLASSICAL ORBITAL TREATMENT OF ROTATIONAL TRANSITIONS IN HEAVY-PARTICLE COLLISIONS (20 min.)
M.R. Flannery and K.J. McCann

F-3 VIBRATIONAL AND ROTATIONAL EXCITATION IN ION MOLECULE COLLISIONS (25 min.)
W. Ronald Gentry and Clayton F. Giese

F-4 KINETIC STUDY OF METASTABLE RARE-GAS ATOMS BY CROSSED MOLECULAR BEAM METHOD (20 min.)
C.H. Chen and Y.T. Lee

SESSION GA: METASTABLE AND EXCITATION TRANSFER

10:45 AM - 12:10 PM, Wednesday, October 22
Ballroom West
Chairman: G.K. Walters, Rice University

GA-1 EXCITATION TRANSFER AMONG THE ^1P_j AND ^3P_j STATES OF Ne* IN SLOW COLLISIONS WITH GROUND STATE Ne ATOMS (7 min.)
N.F. Lane and L.A. Collins

GA-2 ENERGY TRANSFER IN THE CASE OF NO CROSSING POINT (7 min.)
M.G. Payne and M.H. Nayfeh

GA-3 NEW RESULTS FOR EXCITATION TRANSFER IN HELIUM: A STUDY OF RESOLVED $nF \rightarrow 3^{1,3}D$ TRANSITIONS (7 min.)
W.R. Pendleton, Jr., and A.J. Steed

GA-4 VELOCITY DEPENDENCE OF THE VIBRATIONAL BRANCHING RATIO FOR THE REACTION: $Ar^*(^3P_{0,2}) + N_2(X^1\Sigma_g^+, v=0) \rightarrow Ar(^1S) + N_2(C^3\Pi_u, v'=0,1)$ (7 min.)
N. Schweid and E.E. Muschlitz, Jr.

GA-5 KINETIC STUDY OF ENERGY TRANSFER FROM $He(2^1S)$ TO Ar, Kr, AND Xe (7 min.)
M.H. Nayfeh, C.H. Chen, and M.G. Payne

GA-6 DENSITIES OF EXCITED NEON ATOMS IN THE $^3P_2$ (s_5) and $^3P_1$ (s_4) STATES (7 min.)
R.M.M. Smits, M. Prins, and J.A. v.d. Heide

GA-7 DECAY RATES OF $Xe(^3P_1)$ AND $Xe(^3P_2)$ ATOMS AND RADIATIVE LIFETIME OF THE Xe (1_u) MOLECULE (7 min.)
K.F. Palmer, P.K. Leichner, J.D. Cook, and M. Thieneman

GA-8 RADIATIVE LIFETIME OF SOME ROTATIONAL LEVELS OF THE $A^2\Delta$ STATE OF CH (7 min.)
James L. Carozza and Richard Anderson

SESSION GB. LASERS III: CO_2 LASERS

10:45 AM - 12:10 PM Wednesday, October 22
Ballroom East
Chairman: J.T. Verdeyen, University of Illinois

GB-1 LARGE VOLUME SELF-SUSTAINED GLOW DISCHARGES (7 min.)
L.E. Kline and L.J. Denes

GB-2 GAIN IN CO_2 E-BEAM SUSTAINED LASERS (7 min.)
G. Fournier, J. Bonnet, and D. Pigache

GB-3 THERMAL INSTABILITIES IN EXTERNALLY SYSTAINED MOLECULAR LASER DISCHARGES (7 min.)
W.L. Nighan

GB-4 LASER PULSATIONS FROM A FLOWING GAS CW - CO_2 ELECTRIC LASER (7 min.)
M.J. Yoder and D.R. Ahouse

GB-5 CARBON MONOXIDE QUENCHING OF NEGATIVE IONS IN THE CO_2-N_2-He ELECTRIC DISCHARGE LASER (7 min.)
J.F. Prince, W.H. Long Jr., and A. Garscadden

GB-6 A COAXIAL CORONA-PREIONIZED CO_2 LASER (7 min.)
L.W. Casperson and M.S. Shekhani

SESSION HA. HEAVY PARTICLE COLLISIONS II

1:45 PM - 3:20 PM, Wednesday, October 22
Ballroom West
Chairman: W.R. Gentry, University of Minnesota

HA-1 TOTAL SCATTERING CROSS SECTION OF ARGON FROM WATER VAPOR (7 min.)
H.E. Berek and W.R. Snow

HA-2 OBSERVATION OF V-UV RESONANCE LINES EMITTED IN NOBLE GAS ATOM-ATOM COLLISIONS (7 min.)
Robert C. Amme, Harold L. Rothwell and Bert Van Zyl

HA-3 ANOMALOUS VIBRATIONAL STATE DISTRIBUTION IN $N_2^+(B^2\Sigma_u^+)$ AFTER CHARGE EXCHANGE WITH He_2^+ (7 min.)
H.H. Harris, R.J. Pieper, J.D. Earl, and J.J. Leventhal

HA-4 SPECTROSCOPIC STUDIES OF THE CHARGE TRANSFER REACTIONS $He^+ + Hg \rightarrow He + (Hg^+)^*$ and $He_2^+ + N_2 \rightarrow 2\ He + (N_2^+)^*$ AT LOW ENERGIES (7 min.)
Edward Graham IV, Rainer Johnsen and Manfred A. Biondi

HA-5 TOTAL CROSS SECTIONS FOR CHARGE TRANSFER IN COLLISIONS OF He^{++} IONS WITH Ne ATOMS (7 min.)
S.M.L. Prokopenko, P.J. Amick, and T.L. Bailey

HA-6 REACTIONS OF ATMOSPHERIC IONS WITH CF_2Cl_2 AND $CFCl_3$ (7 min.)
F.C. Fehsenfeld, E.E. Ferguson, D.L. Albritton, C.J. Howard, and A.L. Schmeltekopf

HA-7 MICROSCOPIC EXAMINATION OF ION-MOLECULE REACTION MECHANISMS IN ISOTOPIC HYDROGEN SYSTEMS (7 min.)
Charles H. Douglass and W. Ronald Gentry

HA-8 THE EFFECT OF NON MAXWELLIAN H AND F VELOCITY DISTRIBUTIONS IN AN H_2-F_2 REACTION (7 min.)
M. Keith Mätzen and Merle E. Riley

HA-9+ EFFECTS OF ASSUMED PRODUCTION RATES ON CALCULATED DENSITIES IN ELECTRON-IRRADIATED AIR
Merle N. Hirsh

HA-10+ ION CHEMISTRY IN ELECTRON-IRRADIATED AIR: COMPARISON OF EXPERIMENT WITH THEORY
Merle N. Hirsh

+Combined presentation: total time for both papers (10 min.).

SESSION HB. LASERS IV: CO LASERS

1:45 PM - 3:20 PM, Wednesday, October 22
Ballroom East
Chairman: M. Mann, Northrop Research Lab

HB-1 VIBRATIONAL EXCITATION OF CO IN A GLOW-DISCHARGE (7 min.)
J.W. Daiber, H.M. Thompson and T.J. Falk

HB-2 SUBSONIC CW CARBON MONOXIDE ELECTRIC DISCHARGE LASER (7 min.)
T.J. Falk and J.J. Kennedy

HB-3 DISCHARGES IN THE PULSED SUPERSONIC CO LASER (7 min.)
M.F. Weisbach

HB-4 PERFORMANCE CHARACTERISTICS OF A LARGE SCALE SUPERSONIC CO EDL IN PULSED AND QUASI-CW MODES (7 min.)
W.B. Shepherd, W.M. Brandenberg, D.J. Pistoresi and R.L. Haslund

HB-5 SUPERSONIC FLOW ELECTRON BEAM STABILIZED CW CO ELECTRIC DISCHARGE LASER (7 min.)
J.E. Thompson, B.B. O'Brien, C.G. Parazzoli, W.B. Lacina

HB-6 SUPERSONIC CONTINUOUS WAVE CO ELECTRIC DISCHARGE LASER (7 min.)
S.R. Byron, E.L. Klosterman, and T.G. Jones

HB-7 QUASI EQUILIBRIUM VIBRATIONAL POPULATION DISTRIBUTIONS OF ANHARMONIC MOLECULAR LASER SYSTEMS (7 min.)
S.H. Lam and N. Papageorgis

SESSION IA. DISCHARGE STUDIES

3:45 PM - 5:15 PM, Wednesday, October 22
Ballroom West
Chairman: J. Lowke, Westinghouse

IA-1 QUENCHING OF A TRANSIENT PLASMA BY SOLID MICROPARTICLE CONTAMINANT (20 min.)
K. Dimoff and J. Lacoste

IA-2 RELAXATION IN PULSED HELIUM PLASMAS AS INFLUENCED BY PARTICULATE BORON ADDITIVES (7 min.)
E.M. Schnable and Yong Wook Kim

IA-3 ION CONFINEMENT IN LASER-INITIATED PLASMA (20 min.)
J.L. Hirshfield, P. Avivi, I.B. Bernstein, and M.S. Mussetto

IA-4 AFTERGLOW MEASUREMENTS IN KRYPTON AND KRYPTON-NITROGEN MIXTURES (7 min.)
C.J. Tracy and H.J. Oskam

IA-5 RATE COEFFICIENTS FOR THE CHARGE TRANSFER AND PENNING IONIZATION OF N_2 AND CO BY ION AND METASTABLE HELIUM MOLECULES (7 min.)
R.A. Waller, C.B. Collins and A.J. Cunningham

IA-6 PULSED AFTERGLOW STUDIES OF FIVE HELIUM METAL VAPOR LASERS (7 min.)
George Collins

SESSION IB. LASERS V: LASER-RELATED STUDIES

3:45 PM - 5:15 PM, Wednesday, October 22
Ballroom East
Chairman: M. Sexton, University College, Cork (Ireland)

IB-1 FLUORESCENCE EFFICIENCY MEASUREMENTS FROM THE 340 NM BAND OF IODINE IN Ar/I_2 LASER MIXTURES (7 min.)
M.V. McCusker, R.M. Hill, D.L. Huestis, D.C. Lorents, R.A. Gutcheck and H.H. Nakano

IB-2 COLLISIONAL MIXING OF THE LOWEST EXCITED STATES OF Xe_2 AND Ar_2 (7 min.)
R.E. Gleason, J.W. Keto, and G.K. Walters

IB-3 OPTICAL ABSORPTION AND EMISSION IN HIGH PRESSURE Cs-Xe MIXTURES (7 min.)
J.G. Eden, J.T. Verdeyen and B.E. Cherrington

IB-4 THE SEGMENTED HOLLOW CATHODE TUBE AND LASER ACTION IN Cu-He SYSTEM BASED ON SPUTTERING (7 min.)
K.B. Persson, D.L. Franzen, G.J. Collins, G.R. McNeil

IB-5 CHARGE EXCHANGE IN ZINC-NEON (7 min.)
Donald L. Chubb

IB-6 EFFECTS OF COOLING ON A RECOMBINING PLASMA (7 min.)
W.W. Jones and A.W. Ali

SESSION J. WORKSHOP II: ROTATIONAL EXCITATION

7:30 PM, Wednesday, October 22
Manor Inn
Discussion Leader: G. Schulz, Yale University

J-1 SWARM EXPERIMENTS BEARING ON ROTATIONAL EXCITATION
R.W. Crompton

J-2 ROTATIONAL EXCITATION OF MOLECULES BY ELECTRON IMPACT: BEAM METHOD
S.F. Wong

J-3 THEORY OF ROTATIONAL EXCITATION BY ELECTRON IMPACT
E.S. Chang

J-4 THEORY OF ROTATIONAL RESONANCES IN ELECTRON-MOLECULE SCATTERING
Neal F. Lane

J-5 SCATTERING BY MOLECULES WITH A LARGE DIPOLE MOMENT AND THE USE OF THE BORN APPROXIMATION
A. Dalgarno

J-6 ROLE OF ROTATIONAL EXCITATION IN ELECTRIC DISCHARGE LASERS
S.R. Byron

SESSION K. LASERS VI: EXCIMERS AND HIGH PRESSURE LASERS

8:30 AM - 10:00 AM, Thursday, October 23
Ballroom East
Chairman: J. Gerardo, Sandia

K-1+ DISCHARGE MODELING OF THE KrF LASER
J.H. Jacob and J.A. Mangano

K-2+ ELECTRON BEAM CONTROLLED DISCHARGE PUMPING OF THE KrF LASER
J.A. Mangano and J.H. Jacob

K-3 HIGH EFFICIENCY KrF EXCIMER LASER (7 min.)
E.R. Ault, M.L. Bhaumik and R.S. Bradford Jr.

K-4 FLUORESCENCE EFFICIENCY MEASUREMENTS FOR ELECTRON BEAM PUMPED RARE GAS EXCIMERS (7 min.)
C.E. Turner, Jr., P.W. Hoff, J. Taska and L.G. Schlitt

K-5 FORMATION OF XENON DIMERS IN ELECTRON-BEAM-EXCITED XENON AND XENON-NOBLE-GAS MIXTURES (7 min.)
A. Wayne Johnson and James K. Rice

K-6 FORMATION AND DECAY OF XENON DIMERS IN PHOTOEXCITED XENON AND XENON-NOBLE GAS MIXTURES (7 min.)
J.B. Gerardo and A. Wayne Johnson

K-7 THE NITROGEN ION LASER PUMPED BY CHARGE TRANSFER (7 min.)
C.B. Collins, A.J. Cunningham, and B.W. Johnson

SESSION L. BUSINESS MEETING AND INVITED PAPER

10:30 AM - 12:15 PM Thursday, October 23

Mechanical Engineering Auditorium

Chairman: R. Bullis, United Aircraft

THRESHOLD BEHAVIOR OF PHOTON AND ELECTRON IMPACT REACTIONS

F. Read

Manchester University, England

SESSION M. WORKSHOP III: ION MOLECULE REACTIONS

2:00PM - 5:30PM, Thursday October 23
Manor Inn
Discussion Leader: F. Fehsenfeld, National Oceanic and Atmospheric Administration

M-1 MONTE CARLO SIMULATION OF ION MOTION IN DRIFT TUBES
S.L. Lin and J.N. Bardsley

M-2 INFERENCE OF REACTION CROSS SECTIONS FROM DRIFT TUBE MEASUREMENTS OF ION-MOLECULE REACTION RATES

Rainer Johnsen, H.L. Brown, and Manfred A. Biondi

M-3 DRIFT-TUBE STUDIES OF THE EFFECTS OF ION SPEED DISTRIBUTIONS AND INTERNAL ENERGY STATES ON ION MOLECULE REACTIONS
D.L. Albritton, F.C. Fehsenfeld, W. Lindinger, and E.E. Ferguson

M-4 KINETIC THEORY OF ION TRANSPORT AND ION-MOLECULE REACTIONS IN ELECTRIC FIELDS OF ARBITRARY STRENGTH
E.A. Mason and Larry A. Viehland

RECEPTION AND BANQUET
6:30 PM, Thursday, October 23

Social Hour: 6:30 PM
Banquet : 8:00 PM

The Ballroom - The Manor Inn
Chairman: R.H. Bullis, United Aircraft
Speaker : Prof. T. Beveridge, University of Missouri-Rolla

"THEORETICAL AND APPLIED RHABDOMANCY"

SESSION NA. NEGATIVE IONS; BREAKDOWN

8:30AM - 10:15AM, Friday, October 24
Ballroom East
Chairman: J.T. Park, University of Missouri-Rolla

NA-1 PHOTODETACHMENT OF CO_3^- (7 min.)
S.P. Hong and S.B. Woo

NA-2 FORMATION AND DECAY OF SF_6^- (7 min.)
P.J. Chantry and C.L. Chen

NA-3 LOW ENERGY (<3 eV) ELECTRON ATTACHMENT TO C_2H_5Br IN HIGH PRESSURE GASES (7 min.)
R.E. Goans and L.G. Christophorou

NA-4 TEMPORARY NEGATIVE IONS IN UNSATURATED HYDROCARBONS (7 min.)
P.D. Burrow, K.D. Jordan, and J.A. Michejda

NA-5 NET IONIZATION COEFFICIENT IN SF_6 (7 min.)
D.K. Davies

NA-6 MEASUREMENT OF BREAKDOWN POTENTIALS AND TOWNSEND IONIZATION COEFFICIENTS FOR THE PENNING MIXTURES OF NEON AND XENON (7 min.)
A.K. Bhattacharya

NA-7 BREAKDOWN MEASUREMENTS IN MERCURY-ARGON MIXTURES (7 min.)
H.L. Witting

NA-8 CONFIGURATIONAL INSTABILITY IN EXTENDED PLATE-WIRE CORONA (7 min.)
Yong Wook Kim

SESSION NB. TRANSPORT PROPERTIES AND DISTRIBUTIONS

8:30AM - 10:15AM, Friday, October 24
Ballroom West
Chairman: G.L. Rogoff, Westinghouse

NB-1 ELECTRON DISTRIBUTION FUNCTION AND EXCITATION RATES IN N_2 (7 min.)
L.A. Newman and T.A. DeTemple

NB-2 THEORY OF ELECTRON DRIFT VELOCITY MEASUREMENTS IN PARALLEL PLATE GEOMETRY (7 min.)
J.H. Whealton, A.V. Phelps and D.S. Burch

NB-3 THE EFFECT OF ABSORBING BOUNDARIES ON THE DISTRIBUTION FUNCTION FOR ELECTRONS IN A UNIFORM ELECTRIC FIELD IN A GAS (7 min.)
J.J. Lowke, J.H. Parker Jr., and C.A. Hall

NB-4 ELECTRON BOLTZMANN TRANSPORT ANALYSIS OF POTENTIAL ALKALI EXCIMER AND DIMER LASER SYSTEMS (7 min.)
L.A. Schlie and R.P. Benedict

NB-5 THE ELECTRON ENERGY DISTRIBUTION FUNCTION IN ELECTRICALLY-EXCITED MOLECULAR GASES (7 min.)
Manuel Garcia and George Bienkowski

NB-6 THE MOBILITY OF ATOMIC Kr^+ AND Xe^+ IONS IN THE $^2P_{3/2}$ AND $^2P_{1/2}$ STATE IN THEIR PARENT GASES (20 min.)
H. Helm

NB-7 TRANSPORT PROPERTIES OF POSITIVE AND NEGATIVE IONS IN CO_2 (7 min.)
R.Y. Pai, H.W. Ellis, I.R. Gatland, and E.W. McDaniel

NB-8 MOBILITY MEASUREMENTS OF AQUEOUS IONS USING A WILSON CLOUD CHAMBER (7 min.)
Larry E. Stoddard, Paul C. Yue, and James L. Kassner,Jr.

SESSION OA. ISOTOPE SEPARATION AND PHOTON INTERACTIONS

10:30AM - 12:15PM, Friday, October 24
Ballroom East
Chairman: D. Cartwright, Los Alamos

OA-1 PROPOSED PHOTO-SELECTIVE ISOTOPE SEPARATION BY DISSOCIATIVE ELECTRON ATTACHMENT (20 min.)
C.L. Chen and P.J. Chantry

OA-2 COHERENT MULTIPLE PHOTON EXCITATION OF MOLECULES (20 min.)
B.J. Feldman and C.J. Elliott

OA-3 RADIAL CATAPHORESIS OF SELECTIVELY IONIZED ISOTOPES (7 min.)
Gerald L. Rogoff

OA-4 PHOTOIONIZATION OF $6^2P_{3/2}$ CESIUM ATOMS (7 min.)
E.H.A. Granneman, M.J. Van Der Wiel, M. Klewer and K.J. Nygaard

OA-5 THE IMPORTANCE OF HYBRID RESONANCES IN THE MULTIPHOTON IONIZATION OF CESIUM AND RUBIDIUM (7 min.)
D. Popescu, I. Popescu, C.B. Collins, B.W. Johnson, S.M. Curry, M.Y. Mirza, M.A. Tchelemalzadeh, J.A. Anderson

OA-6 RESONANCE IONIZATION SPECTROSCOPY ON He(2^1S) (7 min.)
G.S. Hurst, M.G. Payne, M.H. Nayfeh, J.P. Judish, C.H. Chen, E.B. Wagner, and J.P. Young

OA-7 DIFFUSE RESONANCE SCATTERING OF WHITE LIGHT BY SODIUM (7 min.)
T. Fujimoto and A.V. Phelps

OA-8 VACUUM ULTRAVIOLET ABSORPTION SPECTRA OF HETERONUCLEAR DIATOMIC RARE GAS MOLECULES (7 min.)
D.E. Freeman, K. Yoshino, and Y. Tanaka

SESSION OB. GLOW DISCHARGES

10:30AM - 12:15 PM, Friday, October 24
Ballroom West
Chairman: R. Corbin, University of Missouri-Rolla

OB-1 TWO-DIMENSIONAL, TIME DEVELOPMENT OF PLASMA INSTABILITIES (7 min.)
W.H. Long Jr., and A. Garscadden

OB-2 MAINTENANCE ELECTRIC FIELDS IN A H_2-He dc FLOW DISCHARGE (7 min.)
C.H. Muller and A.V. Phelps

OB-3 CALCULATION OF THE CATHODE REGION OF A GLOW DISCHARGE (7 min.)
G. Fournier and D. Pigache

OB-4 MOLECULAR RADIATION FROM A PURE Hg CONSTRICTED POSITIVE COLUMN (7 min.)
E.R. Mosburg

OB-5 MEASUREMENTS OF THE AMBIPOLAR FIELD IN THE POSITIVE COLUMN OF NEON DISCHARGES (7 min.)
R.M.M. Smits, M. Prins and J.A. v.d. Heide

OB-6 THEORY OF HOLLOW CATHODE ARC (HCA) IN ARGON (7 min.)
J.L. Delcroix, C.M. Ferreira

OB-7 DECAY OF Na-RESONANCE RADIATION IN A Na-Ne AFTERGLOW (7 min.)
M.J.C. Van Gemert and E.A. Bink

SESSION AA

8:30 AM - 10:00 AM, Tuesday, October 21

Ballroom West

ARCS I - FLOW EFFECTS

Chairman: Harold Witting, General Electric

AA-1 Axial Separation of Constituents in Vertically Burning Arcs. E. Fischer, Philips Forschungslaboratorium Aachen, Germany

In most types of arcs burning vertically in a mixture of molecular and atomic gases strong axial segregation of the gas components is observed. A quantitative theory of this phenomenon is given, based on the interaction of diffusion and natural convection. Axial concentration profiles have been calculated for arcs burning in mixtures of mercury with several metal halide additives. A comparison with experimental data obtained from spectroscopic measurements yields good agreement for all mixtures considered. Possibilities of avoiding axial segregation are discussed.

AA-2 Segregation of Minority Species and Constriction of Mercury Arcs Containing Sodium and Scandium Iodides. R. J. ZOLLWEG, Westinghouse Research Labs.--Detailed quantitative measurements have been made of temperature profiles and radial densities of Na, Sc, Sc^+, and I for 5 atmosphere mercury arcs containing sodium and scandium iodides, operated vertically. Sodium is found to be radially demixed in the radiative zone of the arc by a factor of 2-3 and by as much as a factor of 10 over an axial distance of 15 mm. Scandium is segregated radially and axially to a measurable but lesser extent, whereas the segregation of iodine is negligible. Measured radial density distributions are in good agreement with a theoretical demixing model developed by Rogoff, Liebermann and Vine. Measured temperature profiles are somewhat constricted in the upper parts of the arc and are more constricted when "excess" iodine is present ($\sim$200 torr). Theoretically calculated profiles using the energy balance equation and calculated material properties are in reasonable agreement with the measurements. Constriction occurs primarily because of greater net radiation at lower arc temperatures from (1) reduced sodium self-absorption and (2) molecular radiation.

AA-3 Diffusion and Demixing in L.T.E. Plasmas. R.W. LIEBERMANN, G.L. ROGOFF, AND J. VINE, Westinghouse Res. Labs.--Partial pressure gradients and space-charge electric fields can cause alterations of the gas composition (demixing) in multi-element high-pressure arc plasmas. An approach has been developed for calculating radial diffusion velocities of chemically reacting gas components in arc discharge plasmas in local thermodynamic equilibrium (L.T.E.). In this approach specification of the composition at a single location allows the compositions at all other radii to be determined noniteratively. The theory is an extension of that used by Butler and Brokaw[1] for determining the contribution of chemical reactions to the thermal conductivity of gases in chemical equilibrium. Calculations of chemical concentrations have been made for gas mixtures of Hg, I, Na, and Sc (corresponding to vapor lamps), and the results are in better agreement with experimental data[2] than results of the usual approach based on chemical equilibrium neglecting radial demixing. Results of calculations with and without space-charge fields indicate that ambipolar diffusion effects can contribute significantly to demixing.

[1]J.N. Butler and R.S. Brokaw, J. Chem. Phys. 26, 1636 (1957). [2]R.J. Zollweg, This conference.

AA-4 Predictions of Effects of Natural Convection on Vertical Arcs Enclosed in a Tube. J. J. LOWKE, Westinghouse Research Labs. A method has been devised of calculating arc properties in two dimensions including the effect of natural convection from the input material functions of the plasmas. The pressure, temperature axial and radial velocity distributions and axial electric field strengths are derived for any given arc current, electrode separation and cylindrical tube dimensions from the equations of conservation of mass, energy and momentum and also Ohm's Law. Results for 1.5 A in mercury indicate a diffuse arc for a pressure of 1 atmosphere, in agreement with measured temperature distributions, but significant arc constriction is predicted at the lower electrode for 10 atmospheres. The central convective velocity that is derived as a function of axial position for a 2.9 A arc at 1.2 atmospheres in mercury is in good agreement with the experimental results of Kenty.[1] Radial pressure gradients are found to be negligible and the convective flow is predicted to be unicellular in all cases.

1. C. Kenty, Phys. Rev. 9, 53 (1938).

AA-5 Dynamic Temperature Measurements in Ramped Arcs.*D.M. BENENSON and K-J YANG, SUNY/Buffalo -- Temperature measurements have been obtained at various times in ramped d-c arcs which simulate, in part, the current zero behavior of high current a-c plasmas. Experiments were carried out in atmospheric argon in a 1 cm diameter, 15 cm long test section; argon mass flow was 0.1 g/s. Initial current was ∿80A. Following a slowly rising pulse to ∿1,000A, to establish the reference operating condition, the current was ramped through zero using selected values of dI/dt. The dI/dt values ranged from ∿2A/μS to ∿30A/μS. Radial distributions of temperature were obtained at various times within the ramp. Radiation from an argon line (Ar I 4158Å or Ar II 4806Å) and adjacent continuum were simultaneously monitored. Data acquisition time was ∿5μS. At ∿1,000A the centerline temperature was ∿1,900K. For dI/dt ∿ 27 μS, dI_{ℓ}/dt ∿ 10 K/μS, with T_{ℓ} ∿13,000 K at current zero. With dI/dt ∿ 14 A/μS, dT_{ℓ}/dt ∿ 20 K/μS, with T_{ℓ} ∿7000 K at current zero.

*Research supported by National Science Foundation Grant ENG-7415272.

AA-6 Distribution of Electric and Magnetic Quantities in a Moving Arc. * D. BHATTACHARYYA, R. BOLTON, AND M. DROUET, Sciences de base, Institut de recherche de l'Hydro-Québec, Varennes, Québec, Canada, J0L 2P0 - Current density (J), magnetic flux density (B_r, B_θ, B) and force (J x B), and B-flux, effective isobars, and (J x B)-streamlines and their other radial(r) and angular(θ) components are evaluated inside a 1.6 mm long cylindrical arc burning at 700A in air at atmospheric pressure between two parallel copper electrodes and driven at 165 ms^{-1} by a transverse magnetic field of 700G. "Double inversion" method of Olsen et al[1] is used to calculate J from its integrated values - J(x) and J(y), in the directions transverse(y) and parallel(x) to the arc motion as measured on the anode surface by Drouet et al[2]. The arc is elliptical with major axis perpendicular to motion and has long wings. A moment method is developed, starting from J-values, giving analytical series expressions of B_r, B_θ, B and B-flux. Each quantity within the arc boundary is evaluated in two parts contributing from the current flowing inside and outside the zone.

*submitted by C. Richard

[1]H. Olsen, F. Kelly, and L. Price, ARL 69-0061 (1969).
[2]M. Drouet, R. Beaudet, and R. Jutras, AIAA 13, 7 (1975).

SESSION AB

8:30 AM - 10:00 AM, Tuesday, October 21

Ballroom East

LASERS I: ENERGY DEPOSITION IN HIGH PRESSURE GASES

Chairman: R.M. Hill, Stanford Research Institute

AB-1 Transient Vibrational Populations in Excited States of N_2 Under Pulsed Discharge Conditions. D.C. CARTWRIGHT† and N.A. FIAMENGO*.Los Alamos Scientific Laboratory-- The time dependence of the various population processes for the excited electronic states of N_2 have been examined theoretically to determine the relative importance of direct electron impact excitation and intrasystem cascading in establishing the vibrational population of these states. Along with the zeroth vibrational level of the ground electronic state, the vibrational levels of the a', a and w singlet states, and those of the A,B,W,B',C, E, and D triplet states were included. Cascade from higher electronic states is found to be important in determining the vibrational populations in the a' and a singlet and A and B triplet states. Calculation of the inversion densities for various transitions confirm the laser experiment results of McFarlene and suggest identification for previously unidentified laser transitions.

†Los Alamos Scientific Laboratory-supported by the U.S. Energy Research & Development Administration.

*The Aerospace Corporation-supported by the U.S.A.F. SAMSO.

AB-2 Energy Distributions of Electrons in Electron Beam Produced Nitrogen Plasmas.* D. R. SUHRE, and J. T. VERDEYEN, Univ. of Ill., Urbana, IL 61801. A theory was developed which predicts the equilibrium electron energy distributions resulting from the injection of an electron beam into molecular nitrogen. The results were highly non-Maxwellian with a depletion region existing near 2.5 eV. Using these distributions, fractional power transfers to various excitation processes were calculated. The theory was verified experimentally by using Langmuir probes to measure the electron energy distributions produced by a beam generated by a cold cathode discharge in low pressure nitrogen. The distributions were measured in absolute units and compared directly with theory. All of the major features of the theory were found to be present in the measurements.

*Work supported by Division of Physical Research of ERDA.

AB-3 Electron Beam Initiated He-Ne Gas Discharge Laser.* L.A. Newman and T.A. DeTemple, Univ. of Ill.--Recently it has been shown that energy transfer from He metastable states may play a major role in the excitation process of the infrared He-Xe laser (2.026μ and 3.619μ).[1] The possibility for a faster rate of energy transfer between He metastables and Xe has motivated operation at high pressures achieved by utilizing an electron beam initiated gas discharge. This has resulted in a five fold increase in peak output power and nearly doubling the efficiency previously reported. A parametric study of this laser system will be presented of which the significant findings to date are: 1) device limited operation to pressures slightly above one atmosphere 2) peak output power of ≈ 100 kW and 3) an efficiency of ≈ 0.2%

*Work supported by National Science Foundation.

[1]R. Shaker, A. Szoke, E. Zamir and Y. Binar, Phys. Rev. A., 11, No. 4, 1187 (1975).

AB-4 Electron-Beam Excitation of Rare-Gas-Hydrogen Mixtures*. JAMES K. RICE, Sandia Labs --

A very-short-pulse (~ 2 nsec, 440 keV) electron-beam system has been used to excite the $a^3\Sigma_g^+ \rightarrow b^3\Sigma_u^+$ continuous spectrum (~ 3000 Å) of molecular hydrogen. The electron-beam energy is deposited in high-pressure neon (> 10^3 Torr) containing a few Torr of H_2 or D_2. Energy transfer from excited neon populates the $^3\Sigma_g^+$ state (12 eV), which is in turn quenched by collisions with neon at a rate constant of 3×10^{-14} cm^3 sec^{-1} and with H_2 or D_2 at a rate of 5×10^{-11} cm^3 sec^{-1}. Data on the excited-state lifetime and energy-transfer efficiency as a function of neon and hydrogen pressures will be presented.

*Work supported by Energy Research and Development Administration.

AB-5 Fluorescence Emissions from Mixtures of Mercury and Xenon.* JOSEPH R. WOODWORTH, Sandia Laboratories --

Fluorescence emissions have been studied in mixtures of from 0.1 to 9 Torr of Hg and 10 to 150 PSI of Xe in a heated test cell using a relativistic electron beam (0.4 MeV, 12 joules, 3 ns pulsewidth) as an excitation source. Strong band emissions have been observed that extend from 2000 to 2300 Å and from 2537 to 3000 Å. The band starting at 2537 Å was observed to have a decay time at low pressure of 0.75 ± 0.25 microsec. and a fluorescence efficiency of~1%. (Fluorescence efficiency = energy of HgXe photons ÷ e-beam energy deposited in gas.) Pumping mechanisms and possible applications for these emissions will be discussed.

*This work supported by the Energy Research and Development Administration.

AB-6 Electron Energy Distributions in An E-Beam Initiated Xenon Plasma* A.E. GREENE & C.J. ELLIOTT, Los Alamos Scientific Laboratory--Starting with energy deposition by a high energy (10^4eV) beam in an unsustained cavity, the time behavior of the electron energy distribution in a pure Xe gas has been calculated. The initial secondary distribution created by the beam was calculated using the formalism suggested by Green and Sawada[1]. The time evolution of this secondary distribution is then traced using a computer program which solves the linear Boltzmann equation cast into a flux divergent form along the energy axis. Results indicate that nearly all of the secondary electrons created by the energetic primaries are formed at relatively low energies (<100 eV). Subsequent ionizations reduce this secondary distribution to one having an average energy of approximately 4 eV in a picosecond time scale. Beyond this the evolution of the distribution is comparatively slow such that it may be treated as a steady state distribution for many problems of practical interest.

*This work was conducted under the auspices of USERDA.

[1]A.E.S. Green and T. Sawada, J. Atm. and Terr. Phys., 34, 1719 (1972).

AB-7 A Monte Carlo Study of E-Beam Scattering through foils and Gases. Frank T. Wu, Comarco Engr, Ridgecrest, Ca, and Eric A. Lundstrom, Naval Weapons Center, China Lake, Ca. - A Monte Carlo calculation has been made to simulate the keV electron behavior in foil and gas mixtures in a dishcarge for laser devices. A preliminary result has been reported (1) without considering the external electric and magnetic fields. In this study, however, the electric field and the magnetic field are both included in the formulation. The energy deposition and hence the ionization profile are then obtained with the consideration of these external fields. The effects of external fields on the ionization will be discussed.

(1) F.T. Wu and E.A. Lundstrom, Bull .APS 20 235, 1975

AB-8 Modelling of High Pressure Argon-Cesium Discharges.* N. KLEIN, and B. E. CHERRINGTON, University of Illinois, Gaseous Electronics Laboratory, --The two-temperature electron energy distribution approach developed by Vriens[1] has been extended to model high pressure argon (1, 10 atmosphere)-cesium (1 Torr) discharges. A simple three level representation has been used for the cesium and the argon is assumed to act as a buffer gas with the important role of producing Cs-Ar excimers by three body collisions. The important rate coefficients and powers have been calculated as a function of electron density and bulk electron temperature. The results indicate that an electrical discharge in high pressure argon-cesium mixtures can efficiently pump the Cs-Ar excimer (and the possible excimer laser) if the appropriate discharge conditions can be attained.

*This work supported by Los Alamos Scientific Laboratories under subcontract LN5-51449.

[1]L. Vriens, J. Appl. Phys. 44 3980 (1973).

SESSION BA

10:30 AM - 12:00 Noon, Tuesday, October 21

Ballroom West

ARCS II: LTE AND ELECTRODES

Chairman: R.J. Zollweg, Westinghouse Research Labs

BA-1 On LTE in Nitrogen Arcs, J.P. NOVAK and J.P. POULIN, Hydro-Quebec, Institute of Research, Varennes, Quebec. --The intensities of several spectral lines of atomic nitrogen have been measured with the aim of detecting deviations from LTE which were expected to occur for electron densities below $10^{17}cm^{-3}$. The radiation was observed end-on in the current range from 20 to 70 amps. The d.c. arc was generated in a Maecker-type chamber of 5 mm diameter at a pressure of 1 atm. The results have shown that the excited states are in equilibrium for electron densities $n_e \gtrsim 5 \times 10^{16}cm^{-3}$. The temperature obtained from the semilogaritmic plot of the line intensities versus excitation energy agreed with the temperature calculated using the absolute intensity method for the NI4935Å line. Small deviations from linearity in this plot were observed at lower densities. The equilibrium electron density value corresponding to the measured temperature has been compared with the density calculated from the NI4935Å line width. Good agreement was found in the arc center for $n_e \gtrsim 2 \times 10^{16}cm^{-3}$. The agreement is less satisfactory when approaching the arc boundary. The results of our study indicate that LTE exists for $n_e \gtrsim 5 \times 10^{16}cm^{-3}$. The deviations observed below that limit may be due to nonequilibrium effects, however the accuracy of the measurements is not sufficient to draw definite conclusions.

BA-2 The Two-Dimensional, Constant Property Arc.* I. M. COHEN and A. M. WHITMAN, Department of Mechanical Engineering and Applied Mechanics, University of Pennsylvania, Philadelphia, Pa. 19174.--The theory of the (1-dimensional) constant property arc has been extended to a planar arc in two dimensions. This makes use of the canal model where the canal boundary temperature T_*, at which the electrical conductivity jumps discontinuously from zero to a constant value σ_* characteristic of the gas, is specified as a gas property. The Elenbaas-Heller equation is solved for arc temperature distributions subject to Ohm's law and current conservation. Temperatures on the bounding walls and electrodes are specified. The principal parameters of this study are the length (interelectrode distance) to width (between bounding walls) ratio (a) and the conducting spot size (or maximum temperature) on the electrodes (F_o). For $a > 1$, the central plane electric field is nearly coincident with the one-dimensional value. As a increases beyond 2.0, temperature maxima and arc thickness maxima appear near the electrodes. As F_o increases, arc temperatures increase at each point for fixed current.

*Work supported by EPRI.

BA-3 Studies of the Anode Region of a High Intensity Argon Arc*. J. HEBERLEIN and E. PFENDER, University of Minnesota -- Spectrometric studies of the anode region of a constricted, atmospheric pressure argon arc are reported. The arc attaches to a plane, water-cooled copper anode arranged perpendicularly to the axis of the constrictor tube. A spacing of 2.3 mm between the last segment of the constrictor tube and the anode surface permits unobstructed viewing of the anode region. From measured line and continuum emission coefficients, electron temperature and density distributions are derived using two different non-equilibrium data reduction schemes. The results indicate a substantial increase of the electron temperature towards the anode. The electron temperatures show in most cases an off-axis peak.

*Supported by NSF, grant NSF-GK 35230.

BA-4 Study of the Anchored Cathode Spots of a DC Mercury Vacuum Arc. Gisela Eckhardt, Hughes Research Labs--The cathode spot pattern of a dc mercury vacuum arc has been the subject of a photographic study. The cathode[1] consisted of a molybdenum cone which contained a continuously replenished mercury pool and served as an external spot anchor as well. Throughout this study, all spots were anchored at the intersect between molybdenum cone and mercury pool surface, forming a circular pattern around the pool. By varying the mercury feed rate at constant current, the area of the mercury pool (and thus the perimeter length available to the cathode spots for anchoring) can be changed. This made it possible to continuously vary the distance over which cathode spots can spread and to study the effect of this parameter on spot properties. The spots were photographed using an image converter camera in tandem with a four-stage image intensifier tube. Framing and streak photographs revealed a dependence of the average number (and therefore of the current-carrying ability) and average lifetime of the cathode spots on the ratio of mercury pool perimeter to discharge current.

[1] W. O. Eckhardt, U.S. Patent No. 3475 636 (1969)

BA-5 Plasma Interaction with a Rough Wall.
G.H. ECKER, Ruhr-Universität Bochum -
The temperature development of micro-protrusions under the influence of an electric field in the range below the boiling point has been studied in the past. For break-down and arc-electrode phenomena also the evaporation of the tip for higher temperatures and the back reaction of the plasma is of interest. Recognizing the complication of this problem we restrict ourselves to developing scaling laws. Three phases are distinguished: The heating phase, the evaporation phase and the thermal runaway phase. The characteristic time scales for these phases are estimated. Multiple time scale calculation shows that during the evaporation phase up to the runaway point the thermal processes may be considered in quasi-equilibrium. Assuming on the surface a micro-roughness of one characteristic size only the results allow to deduce a model for the cathode spot on the rough surface. The data are in agreement with the findings for the "Type I - spot" by Rakhovsky.

SESSION BB

10:30 AM - 12: Noon, Tuesday, October 21

Ballroom East

LASERS II: NOVEL LASER SCHEMES

Chairman: J. Jacob, Avco Everett

BB-1 Direct Nuclear Pumped Lasers* G.H. MILEY, J.T. VERDEYEN, & W.E. WELLS, University of Ill.-- Recently three laboratories have produced direct nuclear pumped (DNP) lasers (1,2,3,4). These evidences and the available neutron source technology which can provide tens of Megajoules of pumping energy have demonstrated the feasibility of DNP lasers and suggest the possibility of radiation-induced, large-volume, high-power lasers. The studies presented in this paper relate the unique electron distribution function (5,6) produced by radiation induced plasma to the processes of ionization, recombination, charge exchange, and eximer formation. These processes are discussed in terms of the present models for DNP lasers and some predictions for potential lasers given. 1. D.A. McArthur and P.B. Tollefsrud, Appl. Phys. Ltrs., 26, 4, 187 (1975). 2. H.H. Helmick, J. Fuller & R.T. Schneider, Appl. Phys. Ltrs., 26, 6, 328 (1975). 3. R.J. DeYoung, W.E. Wells, J.T. Verdeyen and G.H. Miley IEEE/OSA CLEA 13.A10, Washington, D.C., May 1975. 4. R.J. DeYoung, M.A. Akerman, W.E. Wells, and G.H. Miley, 2nd IEEE Conference on Plasma Science, 75CH0987-8-NPS, May, 1975. 5. R.H. Lo and G.H. Miley, IEEE Trans. on Plasma Science, PS-2, 4, 198 (1974). 6. G.H. Miley, J.T. Verdeyen, and W.E. Wells, ERDA Rpt. #COO-2007-63 (1975).
*This research sponsored by Div. Phys. Res., ERDA.

BB-2 Laser Enhanced Collisional Energy Transfer.* M.G. PAYNE and M.H.NAYFEH,† Oak Ridge Nat'l. Lab. --We consider an effect which has been discussed recently by Harris, i.e., a process in which a photon is absorbed and energy is transferred from one atom to another by way of a collision which occurs in the presence of a laser beam. Under certain resonant conditions (i.e., the laser supplies exactly the right energy photons, and other parameters are correct), the collisional coupling can be so large that a perturbation expansion of the energy transfer amplitude must be summed to all orders in the collisional interaction. This situation is dealt with by solving a three-state model in the limit of slow collisions, leading to the approximate summing of all of the most resonant terms in the infinite order perturbation theory. For collisions with weak coupling, our results reduce to those of Harris.

*Research sponsored by the Energy Research and Development Administration under contract with Union Carbide Corp.

†Postdoctoral research appointment through the Univ. of Kentucky and supported by Los Alamos Scientific Laboratory.

BB-3 Population Iversions in Hydrogen Plasma Nozzle Flows. W. L. BOHN, DFVLR-Institut für Plasmadynamik, Stuttgart, West Germany.-- A Computer study on the occurance of population inversions in atomic hydrogen is presented for a one dimensional nozzle flow at various plasma conditions. Initial electron densities as well as particular nozzle contours drastically change the absolute values of the inversions and their downstream position. The competitive effects of collisional and radiative processes are analysed. The constraints imposed by resonance radiation trapping on population inversions are discussed and demonstrated in numerical examples. All results are compared with quasi steady state solutions and discrepancies are explained in terms of the relaxation time of the first excited level. Finally the possibilities of a plasmadynamic laser with respect to wavelength and coherant radiation power are pointed out.

BB-4 Influence of the electron density on the modes of a pulsed submillimetre laser*, A. HAMONIC AND M.C. SEXTON, University College, Cork, Ireland -- The line emission at 337μ from a pulsed HCN laser (≃ 1 torr, 5kV, 25A for 25μsec) was monitored with pyroelectric detectors. Simultaneous electron density measurements during the lasing action were made with a 8 mm interferometer. Both the asymmetry of the line shape and cyclic variations in output power with pulse frequency strongly indicated the presence of excited HCN molecules up to 20 ms into the afterglow. Moreover, calculations taking radial electron distributions into account supported quantitatively the presence of mode compression near the critical density.

*Work supported in part by the USAF (EOARD) and in part by Culham Laboratory (KAEA).

BB-5 A Very Low Divergence N_2 UV Laser. BRUNO GODARD, Laboratoires de Marcoussis, France --

A very low divergence (0.2 X 0.3 mrad) N_2 UV laser is described ; an intensity of 5 $MW/mrad^2$ was obtained. The average brightness was 2.10^{13} $W/strd \times cm^2$. These results were reached by using a relatively low voltage transmission line with an adequate electrode shape ; the equivalent point source of the laser was determined and the characteristics of the discharge was related to the laser performances.

BB-6 Energy Pathways Following Proton Excitation of Ar-N_2-SF_6 Gas Mixtures.* C. H. CHEN,† J. P. JUDISH, G. S. HURST, and M. G. PAYNE, Oak Ridge Nat'l. Lab. --Time-resolved vuv and visible spectra due to pulsed proton excitation of Ar-N_2 mixtures were measured. It was found that $N_2(C\,^3\Pi_u, v=0,1)$ was primarily excited by $Ar(^3P_2)$, while $N_2(C\,^3\Pi_u, v=2,3)$ was mainly populated by $Ar(^1P_1)$; thus, the Wigner spin conservation rule did not hold rigorously for this system. Various energy transfer mechanisms and their applications to gas lasers are discussed. Time-resolved spectroscopy was also done for N_2-SF_6 and Ar-N_2-SF_6 mixtures because of their relevance to uv lasers. In our interpretation, a small amount of SF_6 can change the distribution of low-energy electrons; thus, the ratio of $C\,^3\Pi_u$ states to $B\,^3\Pi_g$ states in N_2 is increased due to the addition of SF_6.

*Research sponsored by the Energy Research and Development Administration under contract with the Union Carbide Corp.

†Postdoctoral research appointment through the Univ. of Kentucky supported by Los Alamos Scientific Laboratory.

SESSION C

1:30 PM - 3:15 PM, Tuesday, October 21

Ballroom East

ELECTRON COLLISIONS I:

ELECTRON SCATTERING, EXCITATION, AND IONIZATION

Chairman: A. Phelps, Joint Institute for Laboratory Astrophysics

C-1 Momentum Transfer Cross Section for Electron-Argon Collisions. R.W. CROMPTON and H.B. MILLOY, Electron and Ion Diffusion Unit, Australian National University, Canberra. The momentum transfer cross section for electron-argon collisions has been determined in the energy range 0.015 to 6.0 eV by fitting new results for the E/N variation of the electron drift velocity W and the lateral diffusion coefficient D. The minimum in our cross section is shallower and narrower than that derived by Golden from the application of atomic effective range theory to total cross section data but is considerably deeper than the cross section derived by Frost and Phelps from transport data. The present cross section predicts all our W and D data to within 3%.

The validity of the conventional theory used in this work was tested by a Monte Carlo simulation of the drift of an electron in a gas using a cross section with a deep Ramsauer minimum. The results of the simulation are in good agreement with the calculated drift velocities.

The role played by dimers in electron transport coefficient measurements in argon at high pressures will be discussed.

C-2 Experimental and Theoretical Investigation of Diffusion Cooling of Electrons in H_2 -Ar Mixtures. R.W. CROMPTON, T. RHYMES, Australian National University R.E. ROBSON, James Cook University, Queensland. The diffusion cooling of electrons in mixtures of argon and hydrogen has been examined theoretically and experimentally. The Cavalleri electron density sampling technique was used to measure the diffusion coefficient for electrons in mixtures of 0.25, 1, 2, 5, and 10% H_2 in Ar at 4.0 kPa in order to observe the change in diffusion cooling as a function of hydrogen concentration. Theoretical values of the diffusion coefficient in H_2-Ar mixtures were obtained by using a variational technique to solve the Boltzmann equation. In this calculation it was assumed that the momentum transfer cross section for argon was inversely proportional to electron speed and the cross section for hydrogen was constant. The inelastic cross sections used for hydrogen were those obtained by Frost and Phelps using the equations of Gerjuoy and Stein. There is qualitative agreement between the predicted and measured values of the diffusion coefficient.

C-3 Elastic Scattering of Electrons in Molecular Hydrogen. B. VAN WINGERDEN, F.J. DE HEER, E. WEIGOLD*, and K.J. NYGAARD*. FOM-Institute for Atomic and Molecular Physics, Amsterdam, The Netherlands.--Elastic scattering of electrons in H_2 has been studied in the energy range from 100 to 3000 eV and with laboratory scattering angles from 5 to 50°. The results are normalized to the absolute cross sections of Jansen et al.[1] in nitrogen and compared with various theoretical studies and several previous relative experimental measurements.

*Permanent addresses: Flinders University, Bedford Park, South Australia and Univ.of MO,-Rolla, USA, respectively.

[1] R.H.J. Jansen, F.J. de Heer, H.J. Luyken, B. van Wingerden, and H.J. Blaauw, J.Phys. B (in press).

C-4 Electron Excitation of the Sodium Atom. JAMES O. PHELPS AND CHUN C. LIN, Univ. of Wisconsin--Electron excitation functions of the 3^2P and 3^2D states of the sodium atom have been determined by measuring the intensities of the 3^2P-3^2S and 3^2D-3^2P transitions excited by electron impact. The 3^2D state is found to have a much narrower excitation function than the 3^2P state. It has been previously shown that the 3^2D cross sections are markedly influenced by indirect coupling through the P states.[1] Our measured cross sections for 3^2D are in good agreement with the theoretical values obtained by the method of close coupling.[1]

[1] D. F. Korff, S. Chung, and C. C. Lin, Phys. Rev.A 7, 545 (1973).

C-5 Electron Impact Cross Section Measurement of Helium ($2^3S \rightarrow 3^3P$). M. L. LAKE, Universal Energy Systems, Dayton, O. and A. GARSCADDEN, AFAPL, WPAFB, O.--A dual electron beam device is used to measure the excitation cross section for the He $2^3S \rightarrow 3^3P$ levels. Metastables are created by intersecting a neutral atomic beam with a first electron beam operated at 23 eV. The metastables are then excited to the 3^3P state by collision with low energy electrons from a second electron beam, which is modulated. The subsequent modulated 388.9nm emission from the second electron beam region is monitored. Absolute values are obtained by comparison with the direct 3^3P exicitation. Data indicate that $Q(2^3S \rightarrow 3^3P) \sim 1 \times 10^{-17} cm^2$ at 15 eV, as compared to theoretical predictions of $8.2 \times 10^{-17} cm^2$(Born) and $4.4 \times 10^{-17} cm^2$(Eikonal).

C-6 Excitation of the 2A and 3A States of H_2 by Electron Impact* J. Watson, Jr. and R. J. Anderson, University of Arkansas. -- Optical excitation functions have been obtained for several spectral lines corresponding to the 2A→2B and 3A→3B electronic transitions of the neutral H_2 spectrum. The transitions were observed at an effective spectral slit width of ≤2Å over an electron energy range of 0-300eV, and have been identified as originating from the $v' = 2,3,4$, vibrational levels of the 2A state and the $v'=2$ level of the 3A state. In addition, absolute optical cross section measurements have been carried out at 200eV electron energy and 30 mtorr H_2 gas pressure. Theoretical Franck-Condon factors[1] were used with the present data to obtain an estimate of the total apparent cross section for the 2A state.

*Research Supported by the Atmospheric Sciences Section, National Science Foundation.

[1]R. J. Spindler Jr., J. Quant. Spectrosc. Radiat. Transfer. 9, 1041 (1969).

C-7 Measurements of the Electron Impact Ionization Cross Sections of Rb^+ Ions.* R. K. FEENEY, W. E. SAYLE II, and T. F. DIVINE, Georgia Institute of Technology.-- The absolute cross sections for the single ionization of Rb^+ ions by electron impact have been measured as a function of incident electron energy from below threshold to approximately 2000 eV. It was found that the cross section increased from a nominally zero value at and below threshold to a maximum value of about 1.6×10^{-16} cm^2 at an incident electron energy of about 100 eV. In addition there was some evidence of structure in the cross section that was attributed to inner shell ionization. The total error in the measurements was estimated to have a maximum value of less than ±20% with ±10% being typical. Measurements were made in a crossed beam facility operating at pressures less than 10^{-8} Torr. A thermionic-type ion source was used while the electron source employed a thoriated iridium filament pulsed in a manner to produce an electron beam of minimum energy spread. Numerous consistency checks were performed to evaluate possible sources of experimental error.

*Work supported in part by the U.S.E.R.D.A.

C-8 Experimental-Theoretical Comparisons of $1^1S \rightarrow 3^1P_0$, ± 1 Differential Magnetic Sublevel Cross Sections in e-He Scattering*. A. CHUTJIAN, Jet Propulsion Laboratory--

Experimental absolute differential cross sections for the excitations $1^1S \rightarrow 3^1P_0$ and $3^1P_{\pm 1}$ in He will be reported at incident electron energies of 80 eV and 100 eV, and at scattering angles of 10° to 30°. The procedure for obtaining the differential sublevel cross sections (DSCS) is the same as that used previously in the $1^1S \rightarrow 2^1P_{0,\pm 1}$ case[1], using also recent e-photon coincidence measurements in the $1^1S \rightarrow 3^1P$ excitation[2]. Comparisons will be made to DSCS calculated in the 10-channel eikonal[3] and distorted-wave[4] theories.

* Work supported by NASA Contract NAS7-100 to the Jet Propulsion Laboratory.

1. A. Chutjian and S. K. Srivastava, J. Phys. B 8 (1975).
2. M. Eminyan, K. B. MacAdam, J. Slevin, M. C. Standage, and H. Kleinpoppen, J. Phys. B, in press.
3. M. R. Flannery and K. J. McCann, J. Phys. B 8, 1716 (1975).
4. D. H. Madison, private communication.

SESSION DA

3:45 PM - 5:30 PM, Tuesday, October 21

Ballroom West

ARCS III: RADIATION, EMISSION, AND DIAGNOSTICS

Chairman: D.M. Benenson, SUNY/Buffalo

DA-1 Radiation Emission Coefficients for Sulfur Hexafluoride Arc Plasmas. R. W. LIEBERMANN and J. J. LOWKE, Westinghouse Research Labs. Theoretical coefficients for the emission of radiation from the center of cylindrical isothermal plasmas have been derived for temperatures of 5000 to 35,000°K. Because of effects of self absorption of radiation these coefficients are a function of the plasma radius, R, values increasing by a factor of ∿3 as R varies from 2 to 0.1 cm. The emission coefficients were obtained by calculating the total spectral absorptivity including both line and continuum absorptivities, from 100Å to 15,500Å. Line strengths, widths and shifts of approximately 2000 neutral, singly and doubly ionized lines from S and F were calculated using the theory of L-S coupling, except that we used experimental line strengths where they are available. Continuum absorptivities were obtained using the quantum defect method and hydrogenic formula. Plasma composition as a function of temperature was obtained for pressures of 1 and 10 atmospheres using chemical equilibrium theory. At 1 atmosphere line radiation is an order of magnitude greater than continuum radiation and radiation >2000Å is only about 20% of the total radiation for temperatures >15,000°K.

DA-2 Molecular and Excited I^- Continuum Radiation from Metal Iodide Arcs. R. J. ZOLLWEG and R. W. LIEBERMANN, Westinghouse Research Labs.--Quantitative, Abel-inverted, measurements have been made of the continuum radiation at several wavelengths from arcs containing mercury and iodine. Different iodine concentrations were used to distinguish the mechanisms responsible. These radial emission coefficients were compared with equilibrium vapor compositions obtained with a radial demixing model and measured temperature profiles. Molecular radiation from HgI (.4-.45 μm, .7-1.3 μm) and from I_2 (.5-.7 μm) was found in the arc mantle. The arc core contained considerable residual radiation after subtracting recombination radiation and electron-neutral bremsstrahlung from mercury and iodine and Hg_2 molecular radiation. This residual has a threshold near 1.2 μm, extends through the near IR and visible and has a temperature dependence similar to that of the electron or I^+ density. It is attributed primarily to electron attachment to form I^- in an excited state as observed by Neiger[1] in a pure iodine arc. Some modification of Neiger's interpretation is suggested.

[1] M. Neiger, Z. Naturforsch. 30a, 474 (1975).

DA-3 Axis atom density measurements in metal--halide arcs. M. ADRIAANSZ and L. VRIENS, Philips Research Labs., Eindhoven, The Netherlands. -- Electronic Raman scattering from Al and In atoms has been used to determine the absolute densities of these atoms in metal--halide arcs. The arcs contain Hg, I and either Al or In and Tl as main components, have an electrode distance of 40 mm, are enclosed by a 20 mm diam. quartz tube, and were dc operated at 300 to 400 W. The scattering was measured from the arc-axis at 90° with respect to the argon-ion laser beam. The spatial resolution was 1 mm. Al and In atom densities between 10^{16} and 2×10^{17} cm^{-3} have been obtained with inaccuracies of 10 to 30% depending on the discharge conditions. In the analysis use was made of the Raman cross sections determined earlier[1,2].

1 L. Vriens, Optics Commun. 11, 396 (1974).
2 L. Vriens and M. Adriaansz, Optics Commun. 11, 402 (1974) and J. Appl. Phys. 46, 3146 (1975).

DA-4 Optical absorption of tin di-halide molecules as a function of temperature. P.C. Drop and J.H. Verduin Philips, Light Division, Eindhoven, Netherlands.
In high pressure mercury/tin iodide/tin chloride arcs a continuum absorption occurs at wavelengths shorter than 600 nm, due to a layer of SnI_2 molecules near the wall of the discharge tube. When measuring the optical absorption of SnI_2 vapour in a quartz cell placed in an oven at about 800K, rather broad peaks are found[1)], which are not observed when measuring the absorption of the arc. From the behaviour of the absorption after short circuiting the arc, it can be concluded that for certain wavelength regions the absorption is temperature dependent. The effective photon absorption cross section of SnI_2 in the visible and near-UV region has been measured in the temperature range from 900 to 1400K. The absorption peaks are found to broaden considerably with increasing temperature. Extrapolating this data for higher temperatures and combining this with radial temperature measurements in the arc and calculated vapour composition data, the absorption under arc conditions can be calculated. These results are in good agreement with the measurements.

1) R.J.Zollweg and L.S.Frost; J.Chem.Phys. 50 (1969) 3280

DA-5 Measurements of Ly-α and -β Line Profiles in an Argon Arc,* G.L. WEISSLER & HANS-H CARLS, Univ. of So. Calif., Los Angeles.-- In order to check experimentally on the validity of theoretical line shape calculations[1] for atomic hydrogen, the profiles of Lyman-α and -β were measured in the wings of the lines, keeping the plasma temperature and electron density constant. Our arc data (over 100 individual measurements) will be compared to theoretical predictions.[1] Agreement is good in the blue wing of Ly-α and rather poor in its red wing, where measured values were higher than predicted. For Ly-β, only the blue wing could be measured and agreement with theory will be shown to be poor.

*Supported by ONR, Contract #N00014-67-A-0269-0014.
[1]C.R. Vidal, J. Cooper, and E.W. Smith, Astrophys. J. Supplement, series 25, 37 (1973).

DA-6 Temperature Measurements in a Free Burning Arc - S. S. GLICKSTEIN, Westinghouse-Bettis Atomic Power Lab., Pittsburgh, Pa.--The electric arc has been used with much success in welding for many decades, but a comprehensive understanding of the physical phenomenon occurring within the various regions of the arc is still lacking. To provide the base for further study, standard spectroscopic techniques were used to measure the temperature distribution along the axis of a typical argon welding arc of 2 mm arc gap, with a pointed (30°) thoriated tungsten electrode. A cooled copper plate and a Ni-Cr-Fe plate which was allowed to become molten were used as anodes. In both cases the temperature from the cathode to anode ranged from ~11,000°K to ~8000°K for a 100 amp arc. This is significantly smaller than previously reported results for the cooled anode[1], but higher than expected for the molten anode. In addition to the standard argon lines which were used to determine the arc temperature, emission lines from Ni, Cr, and Mn were observed for the case of the molten anode. The temperature T, at the center of the arc was measured for arc currents (I) of 50 to 200 amps and may be approximated by the relation $T = 7643 + 18.8I$°K.

1) Olsen, H. N. Physic of Fluids 2, 614-623 (1959).

DA-7 Non-LTE Spectroscopic Analysis of a Local Fluidized Constriction of a Wall Stabilized Argon Arc*. T. L. Eddy, West Virginia Tech, C.J. Cremers and H.S. Hsia, Univ. of Kentucky.-- A 10 mm dia., 200A, 1 atm cascade arc with a 0.17g/s base flow is constricted radially by a 0.48 g/s flow through a 0.305mm circumferential slot. The resulting non-LTE effects, analyzed with MTE diagnostics presented at prior GEC, indicate axis values tabulated below (in cm, 10^3K, and 10^{17} cm^{-3}) from 6 lines and 5 continuum. Jet distances are from the anode. Values depend on both free-bound and A_H^m values. Schulter's ξ_{fb} and Wende's A_H^m are used below. A_H^m from NSRDS-NBS 22, are 33% larger and give higher T_e and lower T_a values. Morris and Krey experimental ξ_{fb} values decrease N_e and T_e while T_a increases, but much larger std. dev. σ occur between various continuum and arc conditions. With half the A_H^m values in NSRDS-NBS 22 and Schulter's ξ_{fb}, lower T_e, higher T_a and N_e in good agreement with Hβ broad. results.

Location	Position	T_{exa}	$T_{ex\beta}$	T_e	T_a	N_e	($\pm\sigma$)
Upstream	-1	11.0	9.5	30.	3.2	1.2	(13%)
Slot	0	11.6	9.2	41.	2.0	1.3	(16%)
Downstream	+1	12.3	12.1	26.	4.5	1.6	(37%)
Jet 1	12	11.2	10.0	27.	6.6	.9	(5%)
Jet 2	24	10.8	11.1	20.	7.7	.6	(12%)

*Sponsored in part by NSF Grant GK 31453 and the Research, Publication, and Consulting Committee of West Virginia Tech.

SESSION DB

3:45 PM - 5:30 PM, Tuesday, October 21

Ballroom East

ELECTRON COLLISIONS II:

RECOMBINATION AND DISSOCIATION

Chairman: K.J. Nygaard, University of Missouri-Rolla

DB-1 The High Pressure Helium Afterglow at Room Temperature. R.DELOCHE, P.MONCHICOURT, M.CHERET, and F.LAMBERT, CEN/Saclay Fra.--The electron-ion recombination mechanisms of He_2^+ are determined along with the rate coefficients of all the important elementary processes which govern the relaxation of the Helium afterglow at room temperature. A large number of experimental data (atomic and molecular ion currents, atomic and molecular metastable concentrations, electron concentration, elastic electron collision frequency, electron radiation temperature) obtained as a function of time in a wide range of experimental conditions, are compared with the solutions of a system of 5 coupled partial differential equations which includes all the possible processes occuring in an Helium afterglow. A unique set of rate coefficients and constants allowing the precise reproduction of all the experimental data obtained at 7 pressures from 5 to 100 Torr has been found. The recombination rate coefficient for He_2^+ strongly depends on pressure, electron density and electron temperature. The corresponding recombination model is collisional radiative with a dissociation in the lowest excited states leading to the production of atomic metastables. The collisional metastable relaxation rates are in good agreement with available theoretical results.

DB-2 The Importance of Recombination of Molecular Helium Ions in Helium Afterglows.* C.P. DE VRIES & H.J. OSKAM University of Minnesota, Minneapolis. The time dependence of ions, metastable states, and light emission in helium afterglows was measured for pressures from 1 to 30 Torr. The behavior of the $He(^3S)$ metastables and the 10,830 A atomic line demonstrate that recombination of He_2^+ leading to production of $He(^3S)$ metastables is an important process in helium afterglows. This recombination process and metastable-metastable ionizing collisions are included in a three equation model of high pressure helium afterglows. Numerical solutions of these equations for a wide range of recombination and metastable-metastable ionization rates show that the decay of He_2^+ ions in helium afterglows cannot be described by simple ambipolar diffusion, even for late times in the afterglow. Experimental He_2^+ decays confirm the model. They demonstrate the importance of coupling between production of metastables by recombination and production of ions by metastable-metastable collisions. Experimental He_2^+ decays taken in He-Kr mixtures confirm the importance of the coupling.

*Work supported by the National Science Foundation (Grant # ENG-7304157).

DB-3 Rate Coefficients for Excitation of $O_2(b^1\Sigma_g^+)$ by Electrons.* S. A. LAWTON and A. V. PHELPS, JILA, U. of Colorado and NBS--Rate coefficients for electron excitation of the $O_2(b^1\Sigma_g^+)$ state were determined from measurements of the intensity of 762 nm radiation and the lifetime of the $b^1\Sigma_g^+$ molecules in an oxygen filled drift tube. Gas densities of 10^{16} to 2×10^{18} cm^3 result in measured lifetimes of 3 to 30 ms compared to the 12 s radiative lifetime. The excitation rate coefficients increase by a factor of 400 as the electric field to gas density ratio (E/N) is increased from 4×10^{-17} to 10^{-15} V-cm^2. Rate coefficients calculated from electron beam cross sections[1] are much too large for E/N<8×10^{-17} volt-cm^2. For E/N>2.5×10^{-17} volt-cm^2 an approximately linear increase in excitation with E/N is evidence for dissociative excitation of the $O(^1D)$ state followed by efficient excitation transfer to the $b^1\Sigma_g^+$ state. The measured collisional quenching coefficient for the $b^1\Sigma_g^+$ state is 4.5×10^{-17} cm^3 s^{-1}.

*Supported in part by Air Force Cambridge Res. Labs.

[1]S. Trajmar, D. C. Cartwright and W. Williams, Phys. Rev. A 4, 1482 (1971); F. Linder and H. Schmidt, Z. für Naturforsch. 26a, 1617 (1971).

DB-4 Electron Temperature Dependence of Recombination of Electrons with Ammonium Series Ions, $NH_4^+\cdot(NH_3)_n$.* CHOU-MOU HUANG, MANFRED A. BIONDI, and RAINER JOHNSEN, Univ. of Pittsburgh. -- A microwave heating/afterglow/mass spectrometer apparatus has been used to determine the recombination coefficients of electrons with NH_4^+ ions and the cluster ions $NH_4^+\cdot(NH_3)_n$ for n = 1, 2, 3, 4. For measurements where $T_e = T_+ = T$ the values, $\alpha(NH_4^+)$ = (2.5 ± 1), (1.5 ± 0.3), and (1.3 ± 0.2) x 10^{-6} cm^3/sec are obtained at T = 200, 300, 410K, respectively. For the cluster ions, $\alpha(35^+) = \alpha(52^+)$ = (2.8 ± 0.2) x 10^{-6} cm^3/sec at 300K, while $\alpha(69^+) \simeq \alpha(86^+) \simeq$ (3 ± 1) x 10^{-6} at 200K. Over the electron temperature range 300K ≤ T_e ≤ 3500K, both $\alpha(35^+)$ and $\alpha(52^+)$ may be represented by: $\alpha[10^{-6}\ \text{cm}^3/\text{sec}] \simeq (2.8 \pm 0.2)(T_e[K]/300)^{-0.10 \pm 0.02}$, which is a much weaker T_e dependence than that predicted for either the direct or indirect dissociative recombination process.

*This research was supported, in part, by the U.S. Army Research Office (DA-ARO-D-31-124-73G79) and the National Aeronautics and Space Administration (NGR 39-011-137).

DB-5 Dissociation of the Oxygen Molecule by Electron Collision.* SUNGGI CHUNG AND CHUN C. LIN, Univ. of Wisconsin -- The electron-impact dissociation cross sections of the O_2 molecule into $O(^3P)$ and $O(^1D)$ atoms via excitation to the $B^3\Sigma_u^-$ state have been calculated by the Born approximation for the impact-energy range of threshold to 500 eV. The electronic wave functions used in this work have been calculated by employing both single- and multi-configuration with Gaussian-type orbital basis set. Within the framework of the Born approximation the cross sections are computed with full allowence for the variation of the transition moments with respect to the internuclear separation, which makes it possible to asses the validity of the Franck-Condon factor approximation.

*Work supported by Air Force Cambridge Research Laboratories, Office of Aerospace Research.

DB-6 The Dissociative Excitation of the Lyman and Balmer Series of Hydrogen by Electron Impact on CH_4. R. W. MCLAUGHLIN and E. C. ZIPF, U. of Pittsburgh.-- Simultaneous measurements of the absolute intensity of the visible H Balmer lines and the vacuum ultraviolet Lyman Series excited by electron-impact on methane have been made and the absolute magnitude of the excitation cross sections measured from threshold to approximately 400 eV. The methane cross section data have been compared with independent measurements using the same apparatus on the H_2 Werner band system, N_2 singlet transitions and ionized rare gas lines in this wavelength interval. These results form the basis of a convenient extension of the molecular branching ratio calibration technique to the aeronomically important spectral range 900Å to 1215Å, and provide new insights into the mechanism of dissociative excitation.

DB-7 Dissociative Ionization of Cl_2 and HCl by Electron Impact from Threshold to 100 eV.* M.C. MARDEN and W.R. SNOW, U. of Mo-Rolla--Ionization and dissociation of Cl_2 and HCl by electron impact was studied using a mass spectrometer. Ionization curves near threshold and from 0-100 eV were taken of Cl_2^+, Cl^+/Cl_2, HCl^+, Cl^+/HCl, and Cl^{+2}/HCl. The relative ionization cross sections for positive ions formed from Cl_2, HCl, and argon were measured at 75 eV and placed in an absolute scale by normalizing to the total ionization cross section for argon of Rapp and Englander-Golden[1]. At 75 eV the measured cross section for formation of Cl^+ from Cl_2 is $3.3 \times 10^{-17} cm^2$ and for Cl^+ from HCl is $3.5 \times 10^{-17} cm^2$.

*Work supported in part by the Air Force Office of Scientific Research and by the Rolla Metallurgy Research Center of the U.S. Bureau of Mines.

[1]D. Rapp and P. Englander-Golden, J. Chem. Phys. 43, 1464 (1965).

DB-8 Kinetic Energy and Angular Distributions of N^+ from Dissociative Ionization of N_2.* R.J. Van Brunt and L.J. Kieffer, Joint Institute for Laboratory Astrophysics.--Translational kinetic energy and angular distributions of N^+ from dissociative ionization of N_2 have been measured as a function of electron energy. For electron energies above 50 eV the energy distributions agree favorably with earlier data of Kieffer and Van Brunt.[1] Below 50 eV the N^+ distributions are dominated by a feature peaked at an ion energy near 1 eV in agreement with measurements of Locht et al.[2] At the lowest electron energy used the angular distribution associated with the 1 eV feature is consistent with the previously proposed mechanism involving predissociation of the $C^2\Sigma_u^+$ N_2^+ state. At higher electron energies the degree of anisotropy in the angular distributions actually increases before rapidly decreasing with energy suggesting a contribution from direct excitation to the repulsive part of the $^4\Sigma_g^+$ N_2^+ state.

*Supported by the National Science Foundation.

[1]L.J. Kieffer and R.J. Van Brunt, J. Chem. Phys. 46, 2728 (1967).

[2]R. Locht, J. Schopman, H. Wankenne and J. Momigny, Chem. Phys. 7, 393 (1975).

DB-9 Fast Metastable Fragments Produced by Dissociative Excitation of Carbonyl Sulfide. R.J. VAN BRUNT,* Joint Institute for Laboratory Astrophysics, M.J. MUMMA, NASA/Goddard--Electron induced dissociative excitation of OCS has been studied using the method of translational spectroscopy. Time-of-flight distributions and excitation functions of the fast metastable fragments have been measured using different metal surface, Auger-type metastable detectors. The results are compared with similar measurements on CO_2 and show that a variety of metastable fragments including $CO(a^3\Pi)$, $S(^5S)$, $O(^5S)$ as well as various long-lived high-lying atomic and molecular Rydberg fragments can contribute to dissociation.

DB-10 The Dissociative Excitation of H_2, HD, and D_2 by Electron Impact. B. L. CARNAHAN and E. C. ZIPF, U. of Pittsburgh.--Time-of-Flight techniques have been used to study the electron-impact dissociation of H_2, HD, and D_2. Both atomic and molecular metastable species were observed in the TOF spectra of all 3 gases. H_2 and D_2 TOF spectra revealed two distinct features containing mixtures of metastable 2s and long-lived Rydberg atoms, while excitation of HD resulted in 3 atomic features: a fast peak of excited H atoms, a similar atomic D peak, and a broad, slow feature containing both excited H and D atoms. TOF data obtained with the metastable 2s component electrostatically quenched showed that H and D atoms in long-lived Rydberg states were efficiently excited. For H_2 and D_2, the fast atomic peak is ~40% Rydberg atoms, while the slow feature contains less than 10% Rydberg atoms. For HD, Rydberg atoms comprised ~45% of the fast H-atom peak, 35% of the D-atom feature and 20% of the combined slow peak. In HD dissociation the production of Rydberg H atoms is favored over the production of Rydberg D atoms by a ratio of nearly 2 to 1, while the same ratio for H and D atoms in the 2s state is ~ 4 to 3. The preferential excitation of H Rydberg atoms appears to be a consequence of a mass-dependent competition between autoionization and predissociation.

SESSION E

7:30 PM, Tuesday, October 21

Manor Inn

WORKSHOP I: ARC-PLASMA PROCESSING

Discussion Leader: E. Pfender, University of Minnesota

E-1 The Role of Plasma Heaters in the Electric Energy Economy, M.G. FEY, Westinghouse Electric Corp.--In the years ahead, our nation must sharply reduce its dependence upon oil and gas as principal sources of energy. We must shift to an economy based on the consumption of those energy sources which are available -- namely coal and uranium. Utilizing these raw materials will require a shift to electricity as an energy medium, as well as the creation of a large number of high efficiency electrical devices to be used in such areas as transportation, space heating, process steam and direct heating in industry. Plasma heating devices can provide the transition for high temperature industrial applications, and several typical examples are suggested.

E-2 Reactors for Plasma Processing, W.H. GAUVIN, Noranda Research Centre, Canada--With the recent availability of large industrial-scale plasma flame generators, interest in these devices as high-temperature sources is steadily increasing. One of the most promising areas of industrial application involves the contacting of small particles with appropriate plasma tail-flames to effect metallurgical operations. Because of the low particle residence times (of the order of a few milliseconds) available for the reaction, the design of reactors for plasma processing involves a number of interesting features which will be reviewed.

E-3 Plasma Processing in Extractive Metallurgy, D.R. MAC RAE, Bethelem Steel Corporation--Bethelem Steel Corporation has been developing plasma reactor systems for extractive metallurgical processes over several years at the 100 kW and one MW power levels. Potential commercial applications were selected based on the thermodynamic, reaction kinetic, heat transfer and scale-up factors, as well as the short and long term economic implications of electrical intensive processes. Iron ore has been directly converted to molten raw steel continuously in a single plasma reactor operation. This is a promising development which would replace the capital intensive conventional coke works, agglomeration, blast furnace and basic oxygen furnace processes for making steel. In the long term, there are strong incentives to develop an electrical intensive process as an alternative to the present processes which use fossil resources as fuel. In the present development of plasma chemical reactors a basic concept has evolved that the arc heater and chemical reactor system are inseparable as a unit process. As a consequence, for scale-up of a process to a higher power level, a complete development program is anticipated.

E-4 Arc-Coal Process for Converting Coal to Acetylene, R.E. GANNON, Avco-Everett Research Laboratory--An arc-plasma process has been developed for converting coal to acetylene. The viability of the process is due, in part, to the injection of a secondary hydrogen stream into the plasma. An investigation of the role of the hydrogen injection using deuterium and C^{13} tracers showed complete chemical exchange between the primary and secondary stream. A chain mechanism is suggested to account for the complete interchange of atoms.

SESSION F

8:30 AM - 10:30 AM, Wednesday, October 22

Ballroom East

HEAVY PARTICLE COLLISIONS I

Chairman: N. Lane, Rice University

F-1 Rotationally Elastic and Inelastic Collisions of Electrons with Polar Molecules.* F.T. SMITH, D.L. HUESTIS, D. MUKHERJEE, SRI, and W.H. MILLER, U.C. Berkeley.--
A uniform semiclassical S-matrix has been developed for collisions of charged particles with rotating rigid dipoles, making use of first-order perturbation theory. The result is analytical, depending on tabulated functions, and trivial to calculate; it allows evaluation of quantum transitions in classically forbidden regions, and of quantum interference effects. Its main limitation, to collisions at large enough distances for the dipole interaction to be a perturbation, requiring $e\mu/b^2E = 2me\mu/\hbar^2(\ell+\frac{1}{2})^2 \gg 1$, is not a severe restriction for electron collisions at energies near and above 1 eV, where small angle scattering predominates and scattering cross sections are very large. Application to collisions of electrons with alkali halides shows the importance of classically forbidden transitions, demonstrates the failure of some conclusions drawn from Born approximation, and shows the importance of elastic as well as inelastic scattering.

*Work supported by AFCRL, NSF and AFOSR.

F-2 A new multistate semiclassical orbital treatment of rotational transitions in heavy-particle collisions, M. R. FLANNERY and K. J. MCCANN, School of Physics, Georgia Institute of Technology -- A new semiclassical theoretical description of rotational and of vibrational transitions occurring in heavy-particle collisions is presented. The treatment includes appropriate trajectories determined from a certain optical potential designed so as to couple the response of the internal structure to the orbit for the relative motion. Total energy of the system is then conserved. The internal degrees of freedom described by a multistate expansion are closely coupled. The procedure, when applied to various rotational and vibrational transitions in the $H-H_2$, $He-H_2$ and Li^+-H_2 collision-systems, yields integral and differential cross sections in close accord with recent full-quantal calculations. Displays of the resulting angular distributions will be presented for various impact-energies. The present method is extremely useful at impact-energies when many rotational and vibrational channels are open, cases prohibitively difficult for full quantal treatments.

F-3 Vibrational and Rotational Excitation in Ion-Molecule Collisions*, W. RONALD GENTRY‡ and CLAYTON F. GIESE, U. of Minnesota -- We have performed concurrent experimental and theoretical studies of vibrational and rotational excitation in several ion-molecule collision systems. Experimental differential cross sections for resolved quantum vibrational transitions are predicted well by a model which exploits a classical-quantal correspondence principle to permit the use of real classical trajectories (on an accurate potential energy hypersurface) to calculate the probabilities for quantum transitions. The differences in the excitation mechanisms for $H^+ + H_2$, $Li^+ + H_2$ and $H^+ + CH_4$ are interesting and highly instructive.

*Research supported by NSF
‡Alfred P. Aloan Research Fellow

F-4 Kinetic Study of Metastable Rare-Gas Atoms by Crossed Molecular Beam Method. C. H. CHEN† and Y. T. LEE‡, University of Chicago. --The interactions, as well as reactions of a metastable rare-gas atom with ground state atoms or molecules, were investigated with the crossed molecular-beam method which involved the measurements of elastic differential cross sections and ion products. Potential humps are found and determined for $He(2^1S)$-He, $He(2^3S)$-He, and $Ne(^3P_{2,0})$-Ne but not for $Ar(^3P_{2,0})$-Ar, $Kr(^3P_{2,0})$-Kr, and $Xe(^3P_{2,0})$-Xe. The interaction potentials and quenching cross sections were determined for all heteronuclear combinations of metastable and ground state atoms. It was found that quenching cross sections are strongly dependent on collisional energy and the repulsive parts of the interaction potentials. One-dimensional interaction potentials for metastable rare gas atoms with F_2 and Cl_2 were determined. Penning ionization and dissociative process through harpooning mechanism were also investigated.

†Present address: Oak Ridge National Laboratory, Oak Ridge, Tenn. 37830.
‡Present address: University of California, Berkeley, Calif. 94720.

SESSION GA

10:45 AM - 12:10 PM, Wednesday, October 22

Ballroom West

METASTABLE AND EXCITATION TRANSFER

Chairman: G.K. Walters, Rice University

GA-1 Excitation Transfer Among the $^1P_1$ and ^3P_j States of Ne* in Slow Collisions with Ground-State Ne Atoms.* N.F. Lane† and L.A. Collins, Joint Inst. for Lab. Astrophys. and J.S. Cohen, Los Alamos Scientific Laboratory.--The electronic wavefunctions for low-lying states of Ne_2. calculated by Cohen and Schneider,[1] have been used in a close-coupling calculation of excitation-transfer cross sections for the transitions $^1P_1 \rightarrow {}^3P_1$ and $^3P_2$, $^3P_1 \rightarrow {}^3P_2$ and $^3P_0 \rightarrow {}^3P_2$. The spin-orbit interaction is taken to be the dominant coupling leading to transitions. We obtain cross sections at 0.06 eV of 9×10^{-6}, 7×10^{-9}, 2×10^{-3}, and 2×10^{-5} $Å^2$, respectively. All cross sections are found to increase with energy, and in some cases (e.g. $^1P_1 \rightarrow {}^3P_1$) the increase is dramatic. Details of the method will be presented and comparison with experimental rates will be discussed.

*Supported in part by the U.S. Energy Research and Development Administration and the Robert A. Welch Foundation

†JILA Visiting Fellow, 1975-76, on leave from Physics Dept., Rice University, Houston, Texas.

[1]J.S. Cohen and B.I. Schneider, J. Chem. Phys. 61, 3230 (1974).

GA-2 Energy Transfer in the Case of No Crossing Point.* M. G. PAYNE and M. H. NAYFEH,† Oak Ridge Nat'l. Lab. --The classical path treatment of a collision between an excited atom and another atom with a nearly resonant energy level leads to coupled differential equations which have been discussed previously by many workers. We present here an elementary procedure for solving the latter system of equations in the case of no crossing point and in the limit where $\Delta E\tau \gg \hbar$, with ΔE being the energy discrepancy and $\tau = b/v$ being a measure of the time of collision. Even though the method is designed to take advantage of the slowness of the collision, it is also shown to be exact if $\Delta E = 0$. The form of the solution is very similar to that of Vainshtein et al., but the present derivation avoids several of their approximations which individually are not as accurate as their final result.

*Research sponsored by the Energy Research and Development Administration under contract with the Union Carbide Corp.

†Postdoctoral research appointment through the Univ. of Kentucky and supported by Los Alamos Scientific Laboratory.

GA-3 New Results for Excitation Transfer in Helium: A Study of Resolved $nF \rightarrow 3^{1,3}D$ Transitions. W.R. PENDLETON, JR., and A.J. STEED, Utah State University, Logan, Utah, 84322-- Resolved $nF \rightarrow 3^{1,3}D(n=5,6, \&7)$ transitions of HeI have been recorded in spectra induced in low-pressure helium targets by ~100-eV electron impact. The technique of Fourier-transform spectroscopy, utilizing the large throughput-resolution product of a field-widened Michelson interferometer, is currently used in the investigation. The intensity ratios $I(nF \rightarrow 3^3D)/I(nF \rightarrow 3^1D)$ have been investigated over a range of target pressures from 0.5-200 mTorr. The ratios increase rapidly from the low-pressure values of 1.5±0.3 and appear to reach the collisional-equilibrium value of 3 for pressures of ≈0.2 Torr and ≤0.1 Torr for n=5 and (6,7), respectively. Normalization to the absolute $5^1S \rightarrow 2^1P$ cross-section measurements of St. John *et al.*[1] at 100 eV yields a value of $6.0 \times 10^{-21} cm^2$ for the $5F \rightarrow 3^3D$ cross-section in the low-pressure limit. The implications of these observations for excitation-transfer paths in helium will be discussed.

[1]R.M. St. John, F.L. Miller, and C.C. Lin, *Phys. Rev.*, *134*, A888 (1964)

GA-4 Velocity Dependence of the Vibrational Branching Ratio for the Reaction: $Ar^*(^3P_{0,2}) + N_2(X^1\Sigma_g^+, v=0) \rightarrow Ar(^1S) + N_2(C^3\Pi_u, v'=0,1)$.* N. SCHWEID and E.E. MUSCHLITZ, JR., UNIVERSITY OF FLORIDA. --Measurements of the velocity dependence of the branching ratio for the collisional population of v'=0,1 for the title reaction have been performed using a recently completed apparatus, modified to include a monochromator. A beam of Ar* crosses a superthermal N_2 beam and the fluorescence of the N_2* formed is collected, spectrally resolved and signal averaged. By seeding the nitrogen beam, we are able to cover the relative energy range 0.06 to 0.36 ev. Throughout most of this range the branching ratio (v'=0)/(v'=1) is essentially constant at 3.8± 0.2, rising to 4.9± 0.4 at the highest relative energies. The results are compared with the flowing afterglow results of Stedman and Setser[1].

* Supported by the National Science Foundation

1 D. H. Stedman and D. W. Setser, J. Chem. Phys. 52, 3957 (1970).

GA-5 Kinetic Study of Energy Transfer from He (2^1S) to Ar, Kr, and Xe.* M. H. NAYFEH,† C. H. CHEN,† and M. G. PAYNE, Oak Ridge Nat'l. Lab. --Time-resolved vacuum ultraviolet (vuv) emission experiments were done to provide kinetic information on the Jesse effect and, more generally, on the energy pathways applicable to charged particle excitation of helium gas. Our results are consistent with the pathways model of Payne, Klots, and Hurst in which Jesse effects are due primarily to energy transfer from He (2^1S) to an atom or molecule which is consequentially ionized. The results with the time-resolved technique are smaller than theoretical calculations making use of an orbiting approximation, but agree well with experimental data obtained by molecular beam methods. Numerical values of the quenching cross sections are 22.5 $Å^2$, 42.5 $Å^2$, and 57 $Å^2$ for He (2^1S) + Ar, He (2^1S) + Kr, and He (2^1S) + Xe.

*Research sponsored by the U. S. Energy Research and Development Administration under contract with Union Carbide Corp.

†Postdoctoral research appointment through the Univ. of Kentucky and supported by Los Alamos Scientific Lab.

GA-6 Densities of Excited Neon Atoms in the $^3P_2$ (s_5) and $^3P_1$ (s_4) States, R.M.M. Smits, M. Prins, and J.A. v.d. Heide; Univ. of Technology, Eindhoven, The Netherlands--Densities of excited neon atoms in the $^3P_2$ (s_5) and $^3P_1$ (s_4) states have been measured in the positive column of a 100 torr neon gas discharge with currents between 20-120mA using the fluorescence technique. The densities have been determined as a function of the radial position and the discharge current using a tunable c.w. dye-laser. Fluorescence spectra have been measured for different laser input wavelengths. Reaction coefficients for transitions induced by electrons and atoms between the p_2 and p_4 levels have been determined. The results are respectively: $k^e_{2\to4} = 1.6\ 10^{-4}\ cm^3/s$, $k^e_{4\to2} = 2.6\ 10^{-4}\ cm^3/s$, $k^a_{2\to4} = 8.5\ 10^{-13}\ cm^3/s$ and $k^a_{4\to2} = 8.5\ 10^{-13}\ cm^3/s$ for an electron temperature of $3.5\ 10^4 K$ and a gas temperature of 300K.

GA-7 Decay Rates of Xe($^3P_1$) and Xe($^3P_2$) Atoms and Radiative Lifetime of the $Xe_2(1_u)$ Molecule. K. F. Palmer, P. K. Leichner, J. D. Cook, and M. Thieneman, U. of Kentucky.--The time dependence of the vacuum-uv emissions from xenon was studied following low-intensity electron excitation. Collision coefficients for Xe($^3P_1$) and Xe($^3P_2$) atoms and the radiative lifetime of the 1_u molecular state were determined. The de-excitation rate for the transition Xe($^3P_1$) to Xe($^3P_2$) is 9.6 x 10^3 s^{-1}/Torr. The three-body coefficient for $^3P_1$ atoms is 45 s^{-1}/Torr^2. Metastable $^3P_2$ atoms are destroyed in two- and three-body collisions with rate constants 130 s^{-1}/Torr and 39 s^{-1}/Torr^2. The radiative lifetime of the 1_u molecular state is 99 ± 5ns in agreement with the measurement of Keto et al.[1]

[1]J. W. Keto, R. E. Gleason, Jr., and G. K. Walters, Phys. Rev. Lett. 33, 1365 (1974).

GA-8 Radiative Lifetime of Some Rotational Levels of the $A^2\Delta$ State of CH.* JAMES L. CAROZZA and RICHARD ANDERSON, Department of Physics, University of Missouri-Rolla--The radiative lifetimes of some resolvable rotational levels of the v'=0,1, and 2 levels of the $A^2\Delta$ state of CH are measured. Anderson, et. al.[1] with low spectrographic resolution, noted a large variation in lifetime across the $A^2\Delta$ - $X^2\Pi$ band. Our recent data indicates that the rotational levels of the v' = 0 and 1 levels have nearly identical lifetimes between 400 and 500 ns, but the v' = 2 state may have a shorter lifetime by nearly 100 ns.

*The research supported by the Office of Naval Research under grant N0004-14-75C-0477.

[1]Richard Anderson, David Wilcox, Robert Sutherland, Nucl. Inst. and Methods 110, 167 (1973).

SESSION GB

10:45 AM - 12:10 PM, Wednesday, October 22

Ballroom East

LASERS III: CO_2 LASERS

Chairman: J.T. Verdeyen, University of Illinois

GB-1 Large Volume Self-Sustained Glow Discharges* L.E. KLINE & L.J. DENES, Westinghouse Research Laboratories -- We have extended our studies[1] of the formation and operation of UV-preionized, self-sustained glow discharges in CO_2 laser mixtures to homogeneous 10 liter discharges. Measurements of discharge luminosity and laser gain are used to assess the spatial and temporal evolution of discharge uniformity. A preionization model uses an experimental characterization of a single UV-spark to predict the preionization electron density produced by large spark arrays. A discharge initiation model predicts discharge evolution. Comparison of the measured and calculated results shows that 1) a uniform discharge develops even with nonuniform preionization parallel to the electric field, and 2) nonuniform preionization transverse to the electric field leads to a transversally nonuniform discharge. Measured discharge current and voltage vs. time agree well with theoretical predictions and show that the discharge is attachment controlled.

1 L. E. Kline and L. J. Denes, J. Appl. Phys. 46, 1567 (1975).

* Work supported in part by the U. S. Air Force Weapons Laboratory under contract No. F 29601-73-0121.

GB-2 Gain in CO_2 E-beam Sustained Lasers.* G. FOURNIER, J. BONNET, and D. PIGACHE, Office National d'Etudes et de Recherches Aérospatiales (ONERA).-- Predicted time history of small-signal gain is compared with experiments in 9 very different CO_2 laser mixtures (+ pure CO_2) for a wide range of relevant parameters (pressure, electric field/gas density and electron density). An agreement within the experimental errors (better than 20 %) is achieved without any adjustment of the most recently published rate constants (except in pure CO_2 for which a strong current instability is displayed).[2]

*Submitted by J. TAILLET

GB-3 Thermal Instabilities in Externally Sustained Molecular Laser Discharges*. W. L. NIGHAN, United Technologies Research Center.-- An analysis of the factors contributing to glow collapse in externally sustained laser discharges has been carried out for conditions typical of cw, atmospheric pressure CO_2 lasers. The influence of various electron loss processes such as recombination, CO_2 dissociative attachment and three body attachment to O_2 have been examined in detail. Computation of the criterion for thermal instability has shown that these CO_2 lasers are unstable for values of electrical power density in the 100 to 1000 W/cm^3 range. Further, the characteristic time for growth of thermal instabilities at a fixed power density varies from about 10^{-3} to 10^{-4} sec, depending on the nature of the electron loss process. Thus, since the instability growth time is on the order of the flow time in convectively cooled lasers, the electron loss mechanism will significantly affect the occurrence of glow collapse and/or arcing. *Work performed in part through the sponsorship of the Office of Naval Research.

GB-4 Laser Pulsations from a Flowing Gas CW- CO_2 Electric Laser.* M. J. YODER, and D.R. AHOUSE, Avco-Everett Research Laboratory. -- Time resolved laser output flux measurements using a flowing gas CW-CO_2 electron-beam-sustainer electric discharger laser show large fluctuations. Typical laser output at high pressure consists of pulses followed by periods of time during which no flux output is observed. Interferometry simultaneous with power extraction exhibits sharp discontinuities, resembling shock waves in the laser medium. Gain measurements made during lasing show large fluctuations in gain both above and below cavity threshold. A discussion of several physical explanations of this phenomenon is given, and the experimental results are shown to be consistent with a basic self-oscillation mechanism proposed for fast flow CW lasers using unstable resonators.[1]

1 YU. A. Dreĭzin and A. M. Dykhne, JETP Lett. 19, 371 (1974).

*Supported by ARPA/ONR under contract No. N00014-73-C-0363

GB-5 Carbon Monoxide Quenching of Negative Ions in the CO_2-N_2-He Electric Discharge Laser, J.F. PRINCE, W.H. LONG JR., and A. GARSCADDEN, AF Aero Propulsion Laboratory, WPAFB, Ohio---Recent studies show that negative ions play an important role in determining the stability and efficiency of the CO_2 electric discharge laser. Control of the negative ion concentrations is important to the discharge stability and to some extent, the sustaining electric field. With CO_2 or O_2 present, loss of electrons occurs primarily by dissociative attachment, leading to O^-. Our experiments have shown that the O^- clusters rapidly to form other negative ions such as CO_3^-, NO_2^- and NO_3^-. However if CO is present in sufficient quantities, detachment of the O^- is possible. We report direct measurements of the influence of CO on the negative ion concentrations in the CO_2-N_2-He discharge. These experiments were carried out utilizing an on-line mass spectrometer, sampling negative ions in the afterglow directly behind the anode. The total effects and ion concentrations are found to be sensitive functions of discharge current.

GB-6 A Coaxial Corona-Preionized CO_2 Laser. L. W. Casperson and M. S. Shekhani, Univ. of Calif., Los Angeles.--A coaxial discharge TEA laser system has been developed in which the laser radiation propagates along the annular region between a central cathode and an outer cylindrical anode. Since the laser is built into a grounded metal pipe, it possesses improved compactness, ruggedness, and safety characteristics in comparison to conventional glass or Plexiglas housed TEA lasers. Also, the axial symmetry of the current distribution reduces the likihood of arcing. A voltage applied to plastic insulated trigger electrodes prior to the main discharge creates a region of uniform corona ionization near the cathode and delays the onset of arc formation. Detailed information on gas mixtures and discharge conditions will be given. With an active region of 64 cm length and 7.6 cm diameter we have obtained an output power of 15 MW for an input voltage of 25 kV. The resonator mirrors are of a new toric design which localizes the radiation away from the laser axis and permits stable low diffraction modes in spite of the axial obstruction. This discharge technique and resonator configuration are scalable to larger size and may be used with other ionization and sustainer methods.

SESSION HA

1:45 PM - 3:20 PM, Wednesday, October 22

Ballroom West

HEAVY PARTICLE COLLISIONS II

Chairman: W.R. Gentry, University of Minnesota

HA-1 Total Scattering Cross Section of Argon from Water Vapor*, H.E. BEREK and W.R. SNOW, Univ. of Mo-Rolla, Rolla, MO--A seeded supersonic nozzle beam has been used to measure the total scattering cross section for argon from water vapor at relative velocities of 650 to 1100 meters per second. A van der Waals force constant and potential parameters for an assumed Lennard-Jones (12,6) potential have been derived from the velocity dependence of the cross section and the observed "glory" oscillations. The values obtained are

$$C_{app}^{(6)} = 77 \pm 11 \times 10^{-60} \text{ erg cm}^6,$$

$$\sigma = 2.86 \pm .13\text{Å}, \text{ and } \varepsilon = 349 \pm 46 \times 10^{-16} \text{erg}.$$

*Supported by the National Science Foundation, Atmospheric Sciences Section.

HA-2 Observation of V-UV Resonance Lines emitted in Noble Gas Atom-Atom Collisions. ROBERT C. AMME, HAROLD L. ROTHWELL, and BERT VAN ZYL, U. of Denver. -- Vacuum UV emission from Ar-Ar and Kr-Kr collisions has been studied over the center-of-mass energy range of threshold to 150 eV. The neutral atomic beams are formed by both symmetric and nonsymmetric charge-transfer neutralization of an ion beam generated by low-energy electron bombardment. By this procedure, it was possible to observe and to eliminate sizable effects of small quantities of metastable atoms in the neutral beam. Total emission cross sections exhibit an energy dependence quite similar to the respective total ionization cross sections, but are larger in magnitude. The intensity ratio I(106.7)/I(104.8) is about 1.4 for argon atom-atom collisions. For Kr-Kr collisions, we observe I(123.6)/I(116.5) $\simeq$3.7 . These ratios are nearly constant with energy over the intervals measured, viz., 30 to 150 eV and 80 to 150 eV center-of-mass, respectively.

HA-3 Anomalous Vibrational State Distribution in $N_2^+(B^2\Sigma_u^+)$ After Charge Exchange with He^+_2. H.H. Harris, R.J. Pieper, J.D. Earl, and J.J. Leventhal, University of Missouri-St. Louis, St. Louis, Missouri 63121.

Cross sections for $N_2^+(B^2\Sigma_u^+)$ production in 5 eV He_2^+-N_2 and He^+-N_2 collisions are measured by observation of $N_2^+(1N)$ emission. For He_2^+ the cross section is unusually large (~10Å^2) and the vibrational state distribution shows primarily v'=0 and 1, consistent with vertical ionization of N_2. He^+ produces a much wider distribution, as do most other simple ions. Explanations for the large cross section and observed state distributions are proposed.

HA-4 Spectroscopic Studies of the Charge Transfer Reactions $He^+ + Hg \rightarrow He + (Hg^+)^*$ and $He_2^+ + N_2 \rightarrow 2\,He + (N_2^+)^*$ at Low Energies. EDWARD GRAHAM IV, RAINER JOHNSEN and MANFRED A. BIONDI, University of Pittsburgh. -- The reactions $He^+ + Hg \rightarrow He + (Hg^+)^*$ and $He_2^+ + N_2 \rightarrow 2He + (N_2^+)^*$ have been studied in a drift tube-mass spectrometer apparatus fitted with a sapphire window for observing the light emitted from the electronically excited ions. The observation of the 614.9 nm ($7p\ ^2P^o_{3/2} \rightarrow 7s\ ^2S_{1/2}$) transition as the principal emission indicates that the $(Hg^+)^*$ ions are formed in the most nearly energy resonant state, $7p\ ^2P^o_{3/2}$, for which the exoergic energy defect of the reaction is $\Delta\epsilon(\infty) = 0.27$ eV. The emissions observed from the $(N_2^+)^*$ product ions are from the first negative transition ($B^2\Sigma_u^+ \rightarrow X^2\Sigma_g^+$); the most intense lines observed and their corresponding vibrational levels are 391.4 nm (0,0), 427.8 nm (0,1), 470.9 nm (0,2), 522.8 nm (0,3) and 358.2 nm (1,0). The strongest of these lines is the 391.4 nm transition, with only a small intensity ($\lesssim$ 1%) originating from the first vibrational level of the $B^2\Sigma_u^+$ state (358.2 nm), suggesting that undistorted Franck-Condon factors control the N_2 excitation-ionization during the charge transfer.

HA-5 Total Cross Sections for Charge Transfer in Collisions of He^{++} Ions with Ne Atoms*. S. M. L. PROKOPENKO, P. J. AMICK, and T. L. BAILEY, University of Florida--Total cross sections for the formation of He^+ ions in collisions of He^{++} ions with Ne atoms have been measured over the collision energy range 4 - 500 eV. These experiments are of the ion-beam gas-target type, in which the product He^+ ions are separated quantitatively from the projectile He^{++} ions, and from the other ionic collision products, by an electrostatic retardation technique. The cross section ($\sigma[He^+]$) versus collision energy (E) curve is essentially flat from E = 30 eV to E = 500 eV, having an average value of $\sigma[He^+] = 2.5 \times 10^{-16}$ cm^2 over this range. Below E = 30 eV, the $\sigma[He^+]$ versus E curve exhibits some structure, and for $E \leq 14$ eV, $\sigma[He^+]$ increases with decreasing E. The results are discussed in the context of potential curve-crossing theory.

A similar experimental method is being applied to charge transfer in collisions of He^{++} ions with other rare gas atoms, and preliminary results of these experiments will be presented.

*Supported by the U.S. Office of Naval Research

HA-6 Reactions of Atmospheric Ions With CF_2Cl_2 and $CFCl_3$ F.C. FEHSENFELD, E.E. FERGUSON, D.L. ALBRITTON, C.J. HOWARD, and A.L. SCHMELTEKOPF, Aeronomy Lab, NOAA/ERL--The reactions

and $$O_2^- + CF_2Cl_2 \rightarrow Cl^- + CF_2O + ClO \quad (1)$$

$$O_2^- + CFCl_3 \rightarrow Cl^- + CFClO + ClO \quad (2)$$

are found to be fast, $k_1 = 8 \times 10^{-10}$ cm^3/s and $k_2 = 3 \times 10^{-9}$ cm^3/s at 298°K. Both of these reactions are effectively quenched by hydration of the O_2^-. The negative ions CO_3^-, NO_2^-, and NO_3^- do not react with CF_2Cl_2 or $CFCl_3$, $k < 10^{-12}$ cm^3/s. The reaction

$$H_3O^+ + CFCl_3 \rightarrow CCl_3^+ + HF + H_2O \rightarrow CFCl_2^+ + HCl + H_2O \quad (3)$$

has a rate constant 4×10^{-10} cm^3/s. One implication of this is that $\Delta H_f(CCl_3^+) < 196$ kcal/mol or $IP(CCl_3) < 7.7$ eV, substantially less than some previous literature values. Hydrated H_3O^+ does not react efficiently with $CFCl_3$ and H_3O^+ does not react readily with CF_2Cl_2, $k < 10^{-12}$ cm^3/s. The ion NH_4^+ does not react with either CF_2Cl_2 or $CFCl_3$. An important consequence of this investigation is the conclusion that CF_2Cl_2 and $CFCl_3$ molecules are not readily removed by ion reactions in the atmosphere.

HA-7 Microscopic Examination of Ion-Molecule Reaction Mechanisms in Isotopic Hydrogen Systems.* CHARLES H. DOUGLASS and W. RONALD GENTRY‡, U. of Minnesota -- The detailed dynamics of three distinct reaction mechanisms were examined in the following systems containing only hydrogen isotopes:

Abstraction	1.	$H_2^+ + H_2 \longrightarrow H_3^+ + H$	
	2.	$HD^+ + D_2 \longrightarrow D_3^+ + H$	a.
	3.	$D_2^+ + HD \longrightarrow HD_2^+ + D$	b.
	4.	$H_3^+ + D_2 \longrightarrow HD_2^+ + H_2$	
Substitution	5.	$H_3^+ + D \longrightarrow H_2D^+ + H$	
Exchange	6.	$HD_2^+ + HD \longrightarrow D_3^+ + H_2$	

Using a merged-beam technique, we measured the absolute reaction cross sections and product energy distributions over the range of relative kinetic energy ~0.002 eV to 10 eV. Reactions 1-4 all occur by a direct mechanism all energies, but at low energies the evidence indicates that reactions 5 and 6 proceed through the formation of long-lived complexes.

*Research supported by NSF
‡Alfred P. Sloan Research Fellow

HA-8 The Effect of Non-Maxwellian H & F Velocity Distributions in an H_2-F_2 Reaction*. M. KEITH MATZEN & MERLE E. RILEY, Sandia Labs.--

Hot atoms in an H_2-F_2 reaction system are produced by the exothermic linear chain reactions $H + F_2 \rightarrow HF + F$ and $F + H_2 \rightarrow HF + H$ and by the electron beam induced dissociation of F_2. Time-dependent and quasi-steady-state solutions for the velocity distribution functions of H and F atoms lead to an increase in the rates of the chemical reactions that approaches a factor of two larger than the thermalized rates. A complete description of the time dependence of the H and F distribution functions, molecular number densities, and temperature which describe a burning H_2-F_2 system allows the study of the further enhancement of the HF production rate by the hot F atoms produced by the electron beam. The overall burn rate is found to be insensitive to the energy of these F atoms.

*This work supported by the Energy Research and Development Administration.

HA-9 Effects of Assumed Production Rates on Calculated Densities in Electron-Irradiated Air. MERLE N. HIRSH, U. of Minn., Morris -- the AIRCHEM code has been used to calculate the time evolution of ionic and neutral species during a 10^3-second bombardment of airlike N_2:O_2 mixtures at p=2 and 5 Torr and 300°K by 1-MeV electrons. To test the sensitivity of the predictions to assumptions regarding the production rates of specific atomic and molecular ionic and metastable species in collisions of energetic electrons with N_2 and O_2 molecules, three sets of rates currently used by aeronomists were employed, as tabulated below; here Q(X) is the number of X produced per secondary electron. The importance of $Q(N^2D)$ on the buildup of NO and NO_2, and on the resulting behavior of O_3, is demonstrated. Implications to the ion spectra are pointed out. Effects of assumed initial concentrations of NO_2 in the 10^{-7}-10^{-8} range are noted.

Q(X)	N_2^+	O_2^+	N^+	O^+	N^4S	N^2D	O^3P	$O'S$	$O_2'\Delta$	$O_2'\Sigma$
Niles(1970)	.64	.16	.16	.04	.16	.16	.04	.04	.16	.04
Gilmore(1974)	.62	.16	.18	.04	.45	.61	.20	.10	.40	.10
Myers(1974)	.61	.15	.155	.085	.23	.70	.19	.12	.75	.12

HA-10 Ion Chemistry in Electron-Irradiated Air: Comparison of Experiment with Theory. MERLE N. HIRSH, U. of Minn., Morris. -- Ion spectra were obtained during electron bombardment of airlike N_2O_2 mixtures containing traces of H_2O and CO_2, at 2 and 5 Torr, and the results compared with predictions based on AIRCHEM (preceding abstract). Many features of the ion spectra agree with theory. Thus, the ionic composition of the laboratory plasma is as expected; NO^+ builds up and O_2^+ decreases during irradiation as predicted; and the ratios $NO^+/NO^+\cdot H_2O$ and O_4^+/O_2^+ are constant during a given run. Observed discrepancies include unexpectedly large densities of O^- and $NO_3^-\cdot H_2O$, and too small an absolute value for the O_4^+/O_2^+ ratio. The low removal rate for NO^+ previously ascribed to recombination with NO_3^- [1] is shown to involve both NO_3^- and $NO_2^-\cdot H_2O$, resolving the discrepancy with merging beam results. In mixtures containing 342 ppm CO_2, a predicted large density of CO_3^- was not observed. This may indicate the existence of two isomers of O_3^-, one formed by electron attachment to O_3 which reacts slowly with CO_2, and one by clustering of O^- to O_2, the O_2 then switching rapidly with CO_2.

1. P.N. Eisner and M.N. Hirsh, Phys. Rev. Lett. 26, 874 (1971)

SESSION HB

1:45 PM - 3:20 PM, Wednesday, October 22

Ballroom East

LASERS IV: CO LASERS

Chairman: M. Mann, Northrop Research Lab

HB-1 Vibrational Excitation of CO in a Glow-Discharge*+
J. W. DAIBER, H. M. THOMPSON, and T. J. FALK, Calspan Corporation--The efficiency of a continuous glow-discharge for energizing the vibrational mode of CO has been studied. The discharge was operated at supra-atmospheric pressures by the combined use of transverse gas injection through an annular slot in the anode and current limiting of the dc power supply. In a channel having a fixed mass flow and a downstream choked orifice, changes in pressure are a direct measure of heat added to translation. The energy added to vibration was determined by having a second flow channel in series with the discharge, which contained aluminum screening for catalizing the VT relaxation. The energy distribution was inferred from the pressure changes in each flow channel when the discharge was turned on. The fraction of input power deposited in vibration decreased as the input power increased. This is thought to be due to an equilibration of the CO vibration and free-electron energy modes in which superelastic collisions are important. A single curve is found to correlate the energy in vibration with total energy, independent of helium fraction, total pressure or nearness to the arc limit.
*Submitted by J. W. DAIBER
+Work supported by ARPA and AFWL/AFSC

HB-2 Subsonic CW Carbon Monoxide Electric Discharge Laser. -T.J. Falk, Calspan Corp. and J.J. Kennedy, Garrett Corp.--An Electron beam stabilized, transverse flow, electric discharge carbon monoxide laser has been tested in the CW mode. The maximum power loading was equivalent to 0.58 ev/CO molecule. The peak power was 1.1 KW with an efficiency of 17.7 percent. The apparent low signal gains are lower than those predicted in earlier analytical studies.[1,2]. The fraction of the discharge energy which is transferred to CO vibration drops from over 90 percent initially to less than 60 percent for total discharge energies greater than 0.3 ev/CO molecule. This compares favorably with analytical predictions considering the effect of reverse processes on the electron energy distribution.

Submitted by J. Eerkens
Sponsored by United States Air Force, Air Force Systems Command, Air Force Weapons Laboratory, Kirtland AFB, New Mexico
1. AFWL-TR-73-158
2. AFWL-TR-73-187

HB-3 Discharges in the Pulsed Supersonic CO Laser*. M. F. WEISBACH, Boeing Aerospace Co.--Experiments have been carried out to determine the maximum energy loading before the occurrence of the glow-arc transition, in an electron beam sustained discharge for a pulsed supersonic CO laser. The data indicates the parametric performance of the energy loading with gas density, e-beam current density, mixture, and pulse length; the impact on predicted laser performance will be discussed. In addition, voltage-current curves have been measured for various mixtures, and the results agree well with those calculated using measured recombination rates, despite the many nonstandard features of the discharge. Finally, image converter photographs of the arc formation have been obtained and will be discussed.

*Work supported by AFWL Contract No. F29601-73-A-0038-0001.

HB-4 Performance Characteristics of a Large Scale Supersonic CO EDL in Pulsed and Quasi-CW Modes*. W. B. Shepherd, W. M. Brandenberg, D. J. Pistoresi and R. L. Haslund, Boeing Aerospace Co.

A large scale (2.5ℓ optical cavity) supersonic CO EDL has been demonstrated operating in both pulsed and quasi-CW (multiple cavity clearing times) modes. Good agreement was achieved with kinetics code predictions for densities from 0.5 to 1.0 amagat in various CO:Ar:He mixtures for a variety of pulse lengths and power loadings. Scaling of discharge properties of an earlier 0.07ℓ supersonic CO EDL[1] to the larger device will be discussed.

*Work Supported in part by AFWL Contract No. F29601-73-A-0038-0001.

[1]M. F. Weisbach,"Discharges in the Pulsed Supersonic CO Laser." This conference

HB-5 Supersonic Flow Electron Beam Stabilized CW CO Electric Discharge Laser. J. E. THOMPSON, B. B. O'BRIEN, C. G. PARAZZOLI, W. B. LACINA, Northrop Research and Technology Center. A supersonic flow, electron beam stabilized, electric discharge laser has been designed and constructed for quasi-cw operation. The active medium consists of subatmospheric pressure mixtures of CO/N_2, CO/N_2/He, and CO/N_2/Ar supersonically cooled to below $80^{o}K$. A cw output power of 117 kW has been obtained, corresponding to an input power of 618 kW (550 W/cm^3) and an electron gun current density of 2 mA/cm^2. The spatial, spectral, and temporal behavior of the laser output for various electrical excitation and gas medium parameters has been determined and compared with theoretically predicted performance. The supersonic flow quality has also been determined, interferometrically, with and without discharge heat addition.

HB-6 Supersonic Continuous Wave CO Electric Discharge Laser.* S.R.BYRON, E. L. KLOSTERMAN, and T.G.JONES**, Mathematical Sciences Northwest, Inc.--Experimental measurements have been made of the characteristics of an electron-beam-stabilized CW electric discharge laser in various CO gas mixtures at Mach 3.5, 60 °K, and pressure of 0.04 to 0.13 atm. Current-voltage characteristics were taken at electron beam current densities of 0.02 to 1.0 $mamps/cm^2$, showing the transition from attachment-dominated to recombination-dominated loss of electrons. The arc breakdown voltage limit depended strongly on the discharge current applied to the gas as controlled by the electron beam current. Maximum laser power extracted from the 5 cm by 10 cm by 10 cm volume was 60 kW at 18 percent efficiency. Low signal gain measurements on the principal laser emission lines showed lower gain by a factor of about 5 than expected from computer model predictions. The measured reduction in flow Mach number showed that less than 10 percent of the electric discharge power input was converted to gas heating.

*This work was supported by the Air Force Special Weapons Center, Albuquerque, New Mexico.

**T.G.Jones now at Boeing Company.

HB-7 Quasi-Equilibrium Vibrational Population Distributions of Anharmonic Molecular Laser Systems. S.H. LAM and N. PAPAGEORGIS, Princeton University --

The present paper examines the vibrational population distribution for anharmonic molecules. Under the quasi-equilibrium assumption and when the gas is strongly pumped, three distinct regions in the population distribution are identified. Approximate analytical expressions are obtained for the population distribution in these regions that involve only the probabilities P_{vv} and P_{vt} and the translational temperature. The roles of the probabilities in shaping the population distributions are explicitly displayed. Comparison of the approximate analytical expression with "exact" solutions are seen to be quite good.

SESSION IA

3:45 PM - 5:15 PM, Wednesday, October 22

Ballroom West

DISCHARGE STUDIES

Chairman: J. Lowke, Westinghouse

IA-1 Quenching of a Transient Plasma by Solid Microparticle Contaminant. K. DIMOFF and J. LACOSTE, INRS-Energie, U. du Québec - The loading of a large diameter (15cm) argon afterglow (2 torr initial pressure) by nickel microparticles (30μm mean diameter) increases the rate of de-ionization of the plasma by a factor of 50. Despite the application of a pulsed linear discharge to excite the microparticle-gas mixture, the solid phase can be regarded as remaining essentially cold. This results in simultaneous charge density suppression and rapid cooling of the plasma. To account for the solid phase presence, an additional term must be included in each of the three equations which govern time evolution of the heavy gas particle temperature, charge density and electron temperature respectively of the pure discharge[1]. This theoretical model shows good agreement with present observations as well as distinct improvement on simplified theory applied to experimental results obtained elsewhere[2].

[1]K. Dimoff and J. Lacoste, IEEE 2nd Int'l Conf. on Plasma Science, Ann Arbor, Mich. Paper 1C1, (1975).
[2]K. Dimoff and P.R. Smy, Phys. Letters 32A, 13 (1970).

IA-2 Relaxation in Pulsed Helium Plasmas as Influenced by Particulate Boron Additives*. E. M. Schnable and Yong Wook KIM, Lehigh U. -- Relaxation properties of discharge-generated, wall-confined plasmas of helium are studied, with and without particulate boron of a log normal size distribution with maximum at 1.5 μm in dia. Boron is added in a flow of helium (at 2×10^{20} atom/sec, ending in 10^{-4} Torr vacuum) to a concentration of 10^5 particles/cc. For a 20 μsec, 25 J/cc discharge, the final rise to the maximum population in upper atomic levels such as $4s^3S$ shows a rate constant roughly 25% larger than that for ionic levels such as n=4, while in the final decay the ionic rate is larger instead by 25%. In the presence of the boron additives, however, the ionic excitation rate catches up with the atomic rate in the early stage and this holds for the decay as well. The boron additives help increase the excited atomic and ionic populations by as much as 50% under identical discharge conditions. Detailed analysis based on a set of rate equations will be presented.

*Work partially supported by Western Electric Co., Allentown, Penna.

IA-3 Ion Confinement in Laser-Initiated Plasma.* J. L. Hirshfield, P. Avivi+, I. B. Bernstein, and M. S. Mussetto, Yale U.--Experiments[1] indicate that the ions of a laser-produced plasma can be confined well beyond the conventional expansion time by providing intense electron emission from the target. Plasmas of 1 liters volume have been produced by this means with $n > 10^{13}$ cm^{-3} and $\tau > 250$ μsec. An elementary model[2] of a spherical plasma diode is derived in which the ions are confined in a barometric distribution, balanced between the radial inward electric field and the radial outward negative pressure gradient. The model predicts plasma properties in rough agreement with experiment. Extensions of the model to non-spherical geometry, including self-generated magnetic fields, will be discussed. Target mass loss rates in this discharge are of the same order-of-magnitude as in high current vacuum arcs,[3] suggesting applications to material deposition and to ion sources.

*Supported in part by the National Science Foundation.
+Permanent address: The Hebrew University of Jerusalem.
[1]J. L. Hirshfield et al, Physics Letters A (to be pub.).
[2]J. L. Hirshfield and I. B. Bernstein, Physics Letters A (to be published).
[3]C. W. Kimblin, J. Appl. Phys. 44, 3074 (1973).

IA-4 Afterglow Measurements in Krypton & Krypton-Nitrogen Mixtures*. C.J. TRACY & H.J. OSKAM, Univ. of Minnesota-Minneapolis--
The ion species and excited states present in the afterglow of krypton and krypton-nitrogen mixtures have been investigated using a quadrupole mass filter and light emission and absorption spectroscopy. In pure krypton, the pressure dependence of the decay rate for the lower energy metastable state ($1s_5$) was remeasured ($1/\tau = 142/P_o + 87P_o + 32P_o^2; \Lambda^2 = 0.206 cm^2$) as well as the three body atomic ion conversion reaction $Kr^+ + 2\ Kr \rightarrow Kr_2^+ + Kr$ ($k = 2.4 \times 10^{-31} cm^6 sec^{-1}$). This reaction is partly masked by Kr^+ production via mutual metastable collisions. The krypton metastable atom is de-excited by nitrogen; the cross section for this process is $9.0 \times 10^{-17} cm^2$. Two previously undetected ions, KrN^+ and KrN_2^+ were also observed. The former is apparently produced from Kr_2^+ by a reaction with atomic nitrogen ($Kr_2^+ + N \rightarrow KrN^+ + Kr$) and is in turn converted to Kr^+ by the reaction $KrN^+ + N \rightarrow Kr^+ + N_2$. Observations of interest have also been made on the band systems of nitrogen.

*Work supported by the National Science Foundation (Grant #ENG-7304157).

IA-5 Rate Coefficients for the Charge Transfer and Penning Ionization of N_2 and CO by Ion and Metastable Helium Molecules.* R.A.WALLER, C.B.COLLINS and A.J. CUNNINGHAM, U.of Texas at Dallas -- Time-resolved studies of optical absorption and spontaneous emission from mixed gas afterglows at atmospheric pressures excited by intense electron beam discharges can give basic kinetic data on reactions infrequently observed in conventional low-pressure afterglows. This work reports new values of rate coefficients obtained in this way at 300°K for charge transfer reactions of He_2^+ with N_2 and CO of 1.3 and 1.2×10^{-9} $cm^3/sec.$, respectively, for penning ionization of He_2 ($2s^3\Sigma_u^+$) with N_2 and CO of 3.5 and 2.5×10^{-10} and of the polarization molecule (2^3S+1^1S) with N_2 and CO of 1.5 and 1.4×10^{-9} cm^3/sec.

*Research supported in part by ARPA under ONR contract N00014-67-A-0310-0007 and in part by NSF Grant ENG74-06262.

IA-6 Pulsed Afterglow Studies of Five Helium-Metal Vapor Lasers. GEORGE COLLINS, Colorado State Univ.-- Pulsed afterglow studies of five helium-metal vapor lasers indicate that either thermal energy charge transfer,

$$He^+ + M \rightarrow (M^+)^{**} + He, \qquad \text{Reaction a}$$

or Penning ionization,

$$He^M + M \rightarrow (M^+)^{*} + He + e, \qquad \text{Reaction b}$$

is the dominant excitation mechanism. The total velocity averaged cross-sections for both Reaction (a) and Reaction (b) are determined experimentally for the He-Cd, He-Zn, He-I_2, He-Hg, and He-As laser systems.

SESSION IB

3:45 PM - 5:15 PM, Wednesday, October 22

Ballroom East

LASERS V: LASER-RELATED STUDIES

Chairman: M. Sexton, University College, Cork (Ireland)

IB-1 Fluorescence Efficiency Measurements from the 340NM Band of Iodine in Ar/I_2 Laser Mixtures.* M.V. MCCUSKER, R.M. HILL, D.L. HUESTIS, D.C. LORENTS, R.A. GUTCHECK, and H.H. NAKANO, SRI, Menlo Park, California --

We have observed intense band emissions near 340 nm from electron beam pumped mixtures of high pressure argon gas (1 to 6 atm) and iodine vapor (0-2 torr). We identify this emission as arising from transitions between upper ionic states and lower covalent states of molecular iodine. Using the 358 nm band from an Ar/N_2 mixture as a calibration, we have measured the fluorescence yield in this band to be 70±25%; from this we compute an overall fluorescence energy efficiency of 13±4%. Laser action on this band has recently been demonstrated in other laboratories. We will discuss our recent work aimed at developing a kinetic model for this system; an important feature in this model is the role of dissociation and subsequent recombination of the molecular iodine.

* Work supported in part by ARPA through ONR.

IB-2 Collisional Mixing of the Lowest Excited States of Xe_2 and Ar_2.† R.E.Gleason, J.W.Keto✓ and G.K.Walters, Rice University. A low intensity pulsed electron beam is used to study collision-induced transitions between the lowest excited 1_u and 0_u^+ states which are the origin of the vacuum ultraviolet emission from Xe_2^* and Ar_2^*. The rate of the reaction $Xe_2^*(0_u^+) + Xe \rightarrow Xe_2^*(1_u) + Xe$ is found to be $(1.70 \pm 0.28) \times 10^{-13}$ cm^3/sec while that of the reverse reaction is $(7.08 \pm 0.53) \times 10^{-15}$ cm^3/sec at 300°K. The temperature dependence of the latter reaction rate has been used to determine that the 1_u and 0_u^+ states are split by $(888 \pm 92)cm^{-1}$. This result is confirmed by applying the principle of detailed balance to the above reaction. In the case of argon, upper limits of 1.0×10^{-14} cm^3/sec and 1.8×10^{-16} cm^3/sec are established for the rate of the reaction $Ar_2^*(0_u^+) + Ar \rightleftarrows Ar_2^*(1_u) + Ar$ in the forward and reverse directions respectively. These reactions are of importance to models of lasers based on the vacuum ultraviolet emission from rare gases.

†Work supported by Energy Research & Development Admin.

✓Now at University of Texas, Austin, TX.

IB-3 Optical Absorption and Emission In High Pressure Cs-Xe Mixtures.* J.G. EDEN, J.T. VERDEYEN AND B.E. CHERRINGTON, University of Illinois, Gaseous Electronics Laboratory -- The blackbody absorption and flashlamp pumped emission spectra of high pressure Cs-Xe mixtures have shown some new features attributable to CsXe excimers. For $[Xe] \sim 2.7 \times 10^{19}$ cm^{-3} and $[Cs] \sim 2.1 \times 10^{17}$ cm^{-3}, previously unreported absorption was observed to the:

(a) $(Cs[6^2D_{5/2,3/2}]Xe)^*$ (moderate)

(b) $(Cs[7^2S_{1/2}]Xe)^*$ (weak)

and (c) $(Cs[5^2D_{5/2,3/2}]Xe)^*$ (strong)

excimer states. Also, utilizing Xenon flashlamp pumping, dominant $(CsXe)^*$ emission was observed in the vicinity of 6900 Å, corresponding to transitions from the $(Cs[5^2D_{5/2,3/2}]Xe)^*$ state to ground. In contrast, Tam et al[1] observed intense $(Cs[7^2S_{1/2}]Xe)^* \rightarrow (Cs[6^2S_{1/2}]Xe)$ fluorescence due to selective excitation of Cesium by an argon ion laser. The relationship of these results to potential CsXe excimer lasers will be discussed.

*Work supported by NASA Lewis Research Center.

[1]A. Tam, G. Moe, W. Park, and W. Happer, Phys. Rev. Lett. 35, 85 (1975).

IB-4 The Segmented Hollow Cathode Tube and Laser Action in Cu-He System Based on Sputtering K.B. PERSSON, D.L. FRANZEN, NBS and G. J. COLLINS, G. R. MC NEIL, CSU-A hollow cathode has been designed to produce continuous high power negative glow plasmas. Input powers of 500 to 1500 watts per cm of plasma length have been achieved. This level of input power compares favorably with the higher power, positive column ion laser plasmas. The rate of sputtering at these power densities generates vapor densities of the cathode material high enough to be useful as a laser medium. The Cu-He system, obtained with Cu electrodes and He buffer gas, is a good illustration. An 80 cm long discharge tube with a diameter of 2 cm has produced an output power of 100 mW at 7808 Å with an input of 20 kW. This transition, $6s\ ^3D_3 \rightarrow 5p\ ^3F_4^0$ in the Cu ion state system, is probably generated by the charge transfer reaction $(He^+ + Cu = Cu^{+*} + He)$. An effective charge transfer cross section of about 10^{-14} cm^2 was inferred from spatial measurements of the neutral copper vapor density. Considering the non-optimized cavity output coupling of only 1%, and the scaling laws for the plasma; the 80 cm tube should be capable of powers from 1 to 10 watts which compares favorably with present ion lasers.

IB-5 Charge Exchange in Zinc-Neon. DONALD L. CHUBB NASA Lewis Research Center.--Charge exchange between Ne^+ and Zn is a possible mechanism for preferentially populating the 4d and 5p levels of Zn^+ and therefore producing an inversion. A low power flowing Ne plasma was seeded with Zn to determine if charge exchange or electron collisional excitation is the dominate pumping mechanism for the 4d and 5p levels. Spontaneous emission intensities proportional to the densities of the 4p, 5s, and 4d levels were measured. From the dependence of the intensity ratios 4d/4p, 4d/5s, and 5s/4p on input power it is possible to deduce whether charge exchange or electron excitation is the dominate pumping mechanism of the 4d and 5p levels. Results indicate that predominate charge exchange pumping exists for the $4d^2D_{5/2}$ level only. Data in Zn-Ar are compared with the Zn-Ne results. The intensity ratios $4d^2D_{3/2}/5s^2S_{1/2}$ and $4d^2D_{5/2}/5s^2S_{1/2}$ were nearly the same in Zn-Ar as is expected for electron pumping. However, in Zn-Ne the $4d^2D_{5/2}/5s^2S_{1/2}$ ratio was nearly twice the $4d^2D_{3/2}/5s^2S_{1/2}$ ratio. Since electron pumping cannot account for this result, it was concluded that charge exchange is the dominate pumping mechanism for the $4d^2D_{3/2}$ level.

IB-6 Effects of cooling on a recombining plasma. W.W. JONES 7 A.W. ALI, Naval Research Laboratory--Previously[1] we studied the population inversion found during the initial phases of a recombining plasma of bare nuclei and free electrons. In this early phase of the recombination, lasing action of each atomic level pair terminates in a time less than the radiative life time of that pair of atomic levels. This stage is relevant to very short wavelength lasers. Steady state is then established amongst the excited states. Subsequent cooling of the plasma disturbs this steady state distribution and further inversion between levels can occur. Several cooling schemes are studied and inversion densities and gains are calculated. These schemes can be employed to cool the plasma as a prerequisite for realization of a plasma dynamic laser.

[1]W. W. Jones and A. W. Ali, Appl. Phys. Lett. 26, 450 (1975).

SESSION J

7:30 PM, Wednesday, October 22

Manor Inn

WORKSHOP II: ROTATIONAL EXCITATION

Discussion Leader: G. Schulz, Yale University

J-1 Swarm Experiments Bearing on Rotational Excitation. R.W. CROMPTON, Research School of Physical Sciences, Canberra, Australia--Swarm Experiments provided early evidence for direct rotational excitation by electron impact, and were subsequently developed as a method for determining rotational excitation cross sections. In some circumstances it has been possible to determine absolute cross sections by this method; in others it has provided tests of the validity of theoretically devised values. Since the cross section data must be unfolded from experimental measurements that relate to a distributed range of electron energies and to more than one type of collision process, the questions of uniqueness and accuracy can only be examined against a background of the basic concepts underlying the method. Some examples will be given to illustrate these concepts as well as to demonstrate both types of application referred to above. A comparison will be made between the results of swarm experiments and the predictions of Modified Effective Range Theory taking account of rotational excitation, and a description given of the experimental measurements that relate to the suggestion of 'rotational resonances'.

J-2 Rotational Excitation of Molecules by Electron Impact: Beam Method. S.F. WONG, Yale U -- Experimental studies on rotational excitation in H_2 and N_2 by low energy electrons using crossed-beam techniques are reviewed. In H_2, we have available data on rotational excitation, $\Delta j=2$ in the energy range 0.5-100 eV and angular distributions associated with vibrational transitions v=0-1, 0-2 and 0-3. Theory is generally in good agreement with experiment. In N_2, rotational transitions $\Delta j=2$ and $\Delta j=4$ have been deduced from beam experiments in the energy range 1-4 eV. The angular dependencies have also been measured. As in the case of pure vibrational excitation, resonances play an important role in rotational excitation as well.

J-3 Theory of Rotational Excitation by Electron Impact. Edward S. Chang, University of Massachusetts, Amherst --Besides clarifying the relationship between the close-coupling and the adiabatic-nuclei theories, the frame-transformation theory[1] points the way to an economical calculation in certain circumstances. Calculational results which account for simultaneous vibrational as well as rotational excitation in $e - H_2$ at a few eV are discussed and compared to experiment.

[1] E.S. Chang and U. Fano, Phys. Rev. A6, 173 (1972).

J-4 Theory of Rotational Resonances in Electron-Molecule Scattering. N. F. Lane,* Joint Inst. for Lab. Astrophysics.--The theory of rotational resonances[1] is briefly described and the results of calculations[2] reviewed. Principal supportive and critical theoretical arguments are discussed and alternative schemes are outlined.

*JILA Visiting Fellow, 1975-76, on leave from Physics Dept., Rice University, Houston, Texas.

[1]L. Frommhold, Phys. Rev. 172, 118 (1968).

[2]D. J. Kouri, J. Chem. Phys. 49, 4481 (1968): W. R. Garrett, Phys. Rev. A 11, 509 (1975); Abstracts of Papers of IXth ICPEAC, vol. I, ed. by J. S. Risley and R. Geballe (Univ. of Wash. Press, 1975); p. 257.

J-5 A. DALGARNO, Center for Astrophysics, Harvard College Observatory and Smithsonian Astophysical Observatory.--The scattering of electrons by molecules with large dipole moments is discussed and the usefulness of the Born approximation for the calculations of total and momentum transfer cross sections is assessed.

J-6 Role of Rotational Excitation in Electric Discharge Lasers. S. R. BYRON, Mathematical Sciences Northwest, Inc.--The role of rotational excitation in various molecular laser systems is reviewed. The systems that are most susceptible to rotational effects are those based on molecules containing light atoms (H or D) and those based on partial inversions. The importance of rotational excitation of H_2 by electron impact is illustrated by calculations of the laser characteristics of the H_2-HF transfer electric discharge laser. The sensitivity of laser performance to quite small rotational cross-sections is illustrated by a parametric analysis of the characteristics of the supersonic CO electric discharge laser. Related experimental measurements for these laser systems are also discussed.

SESSION K

8:30 AM - 10:00 AM, Thursday, October 23

Ballroom East

LASERS VI: EXCIMERS AND HIGH PRESSURE LASERS

Chairman: J. Gerardo, Sandia

K-1 Discharge Modeling of the KrF Laser*
J. H. JACOB and J. A. MANGANO, Avco-Everett Research Laboratory, Inc., Everett, MA--Preliminary modeling of the electron-beam stabilized discharge used to pump the KrF laser has been carried out. The model includes electron impact excitation and ionization of the ground and metastable states of Kr. The rare gas metastables are atomically similar to the alkalis so we have assumed that the electron impact cross-sections of the metastables are the same as the alkalis. We find metastable ionization to be the dominant ionization rate. Further, the electrical efficiency of producing the metastables is a strong function of the fractional metastable population.

*This research was supported by the Advanced Research Projects Agency of the Department of Defense and was monitored by ONR under Contract No. N00014-75-C-0062.

K-2 Electron Beam Controlled Discharge Pumping of the KrF Laser* J. A. Mangano and J. H. Jacob, Avco Everett Research Laboratory, Inc., Everett, MA --

Laser action has been obtained in atmospheric pressure mixtures of 0.3% F_2/6% Kr/97.9% Ar at 248.5 and 249.5 nm with electron beam controlled discharge pumping. The laser and discharge characteristics are explored as a function of electron beam current density, discharge electric field and laser mixture pressure. Measurements of laser output energy, pulse length and electric efficiency will be presented. Implications of these results in terms of the eventual intrinsic electrical efficiency achievable will be discussed.

*This research was supported by the Advanced Research Projects Agency of the Department of Defense and was monitored by ONR under Contract No. N00014-75-C-0062.

K-3 High Efficiency KrF Excimer Laser.* E. R. AULT, M. L. BHAUMIK and R. S. BRADFORD, JR. Northrop Research and Technology Center. -- Efficient, high power laser emission has been observed at 249 nm from a KrF excimer laser obtained by an E-beam pumped mixture of Ar, Kr and NF_3 (1300:130:1) at a total pressure of 2.25 atm. An energy of 2.3J was extracted in a 125 nsec (FWHM) pulse from a 100 cm^3 volume using a coaxial E-beam laser. Laser efficiency was estimated to be nearly 23% based on energy deposition in the gas.

*Research supported by ARPA/ONR under Contract N00014-72-C-0456.

K-4 Fluorescence Efficiency Measurements for Electron Beam Pumped Rare Gas Excimers. C.E. Turner,Jr., P.W. Hoff J. Taska and L.G. Schlitt, Lawrence Livermore Laboratory. -- High absolute efficiencies (10-30%) measured for 250kV, few A/cm^2 pumping of VUV continua at 1-3 atm correlate well with excimer kinetics codes and may permit efficient photolytic pumping of group VI metastables [e.g.,$O(^1S)$, $S(^1S)$] as fusion lasers. The efficiencies were measured by techniques designed to overcome serious deficiencies of differential calorimetry or simplistic schemes such as the use of Berger-Seltzer dE/ds tables for energy deposition. Photodiodes with measured absolute spectral response were used in a well defined lens/pinhole geometry that permitted calculation of the effective radiating volume viewed. Spatially resolved calorimetry was performed at the cell foil to characterize the distribution of energy in the incident electron beam. With this data as input for a 3-D Monte Carlo electron transport code (SANDYL), the spatial distribution of energy deposition in the gas was calculated taking into account multiple scattering and cell geometry. The validity of the SANDYL technique is substantiated by excellent agreement with calorimetric energy flux measurements at various depths in the gas.

* Work performed under the auspices of the U.S.E.R.D.A.

K-5 Formation of Xenon Dimers in Electron-Beam-Excited Xenon & Xenon-Noble Gas Mixtures*. A. WAYNE JOHNSON & JAMES K. RICE, Sandia Labs.--

The formation rate of electron-beam-excited Xe_2^* (1720-Å radiation) is markedly increased by the addition of helium and argon to the xenon. The phenomenological effect is distinct and easy to document. A complete accounting of all the rates is not possible at this time. However, under certain conditions, the association rate of $Xe_2^*(^1,^3\Sigma_u^+)$ from three-body collisions of Xe^*, Xe, and R (where R is a noble gas atom) determines the growth time of the 1720-Å continuum radiation. We have interpreted the data in terms of these association rates and obtained rate constants of 5.0, 1.4, and 2.3 (10^{-32} cm^6 sec^{-1}) for xenon, helium, and argon respectively as the third body.

*This work supported by the Energy Research and Development Administration.

K-6 Formation & Decay of Xenon Dimers in Photoexcited Xenon & Xenon-Noble Gas Mixtures*. J.B. GERARDO & A. WAYNE JOHNSON, Sandia Labs.--

Associative combination rates for the formation of an excited diatomic xenon molecule from a xenon metastable atom, a ground-state xenon atom and a third body of either xenon or another noble gas atom are reported. The xenon metastable atoms are formed by photoexciting xenon gas with a 10-nsec-wide pulse of 1460 ± 10 Å laser radiation from a krypton-dimer laser. The temporal dependence of the spontaneous emission of the excited xenon dimers is fitted to a kinetic model to obtain formation rates and lifetimes. The associative combination rates found in this manner are from 20 to 50% higher than the rates measured with intense electron-beam excitation - the apparent reason for this difference is discussed. The inferred lifetimes distinctly show that two xenon dimer states are formed. The two states have radiative lifetimes on the order of 5 nsec and 100 nsec, which is in agreement with other studies.[1]

*This work supported by the Energy Research and Development Administration.

[1]J. W. Keto, R. E. Gleason, Jr., and G. K. Walters, Phys. Rev. Letters 33, 1365 (1974).

K-7 The Nitrogen Ion Laser Pumped by Charge Transfer.* C.B. COLLINS, A.J. CUNNINGHAM, AND B.W. JOHNSON, U. of Texas at Dallas -- The scaling to high powers of the nitrogen ion laser pumped by charge transfer from molecular helium ions has been accomplished. Three laser lines have been individually excited at 3914, 4278 and 4709 Å upon discharge of a fast-pulsed electron beam gun APEX-1, into several atmospheres of a mixture of helium and nitrogen. Excitation current densities were varied from 1.4 to 3.5 KA/cm^2 at 1 MV over a 1 x 10 cm transverse geometry. The efficiency of the 4278 Å laser emission was found to be proportional to the total pressure raised to the 1.2 power. Outputs of 36 mJ have been obtained from the 16 cc working volume at 30 atm. pressure and a peak efficiency of 1.6% relative to the energy lost by the electron beam in this radiating volume has been achieved.

*This research was supported by the U.S. Advanced Research Projects Agency of the Department of Defense and monitored by ONR under contract No. N00014-67-A-0310-0007.

SESSION M

2:00 PM - 5:30 PM, Thursday, October 23

Manor Inn

WORKSHOP III: ION MOLECULE REACTIONS

Discussion Leader: F. Fehsenfeld, NOAA

M-1 Monte-Carlo Simulation of Ion Motion in Drift Tubes.*
S. L. LIN and J. N. BARDSLEY, University of Pittsburgh.-- The Monte Carlo method, in which the motion of a typical ion through several hundred thousand collisions is simulated, has been used to relate transport properties, such as mobility and diffusion coefficients, to the cross sections for collisions of the ions with buffer gas atoms or molecules. For monatomic systems the cross sections are in turn determined by the interaction potential. In the course of a Monte Carlo calculation one also generates the ion velocity distribution. For several systems, including O^+ in He, O^+ in Ar and O^- in He, we have derived interaction potentials which are consistent with the observed mobilities. The corresponding velocity distributions have been used in the analysis of the drift-tube measurements of various reaction rates by Johnsen et al. and Albritton et al. The Monte Carlo approach should also be valuable in providing tests for analytic solutions of the Boltzmann equation, and in determining the extent of the information that can be deduced from drift tube experiments.

* Supported, in part, by the Army Research Office.

M-2 Inference of Reaction Cross Sections From Drift Tube Measurements of Ion-Molecule Reaction Rates*.
RAINER JOHNSEN, H. L. BROWN** and MANFRED A. BIONDI, University of Pittsburgh. -- In order to obtain the velocity dependence of ion-molecule reaction cross sections from drift tube measurements it is necessary to carry out a "deconvolution" of the measured rate constants. As an example of such a procedure, we have applied ion-velocity distributions (obtained by Bardsley and Lin from Monte Carlo computations) to our drift tube data on the endothermic charge transfer reaction $O^- + O_2 \rightarrow O + O_2^-$. The reliability of the inferred cross section is demonstrated by computing rate constant data for various assumed cross section models and comparing these with the measured data. In addition, attempts to obtain velocity distributions of drifting ions by experimental methods, in particular by retarding potential measurements performed on the ions effusing from the drift cell, will be discussed.

*Supported, in part, by the Army Research Office.
**Present address: Stanford Research Institute, Menlo Park, California.

M-3 Drift-Tube Studies of the Effects of Ion Speed Distributions and Internal Energy States on Ion-Molecule Reactions*, D. L. ALBRITTON, F. C. FEHSENFELD, W. LINDINGER**, and E. E. FERGUSON, NOAA Environmental Research Laboratories.--Being a suprathermal swarm technique, the drift-tube is well-suited to examine the energy dependence of ion-molecule reactions in the important range from 300°K to a few eV. However, the interpretation and use of such data are complicated by (a) the generally unknown, non-Maxwellian ion speed distribution and (b) the possibility of field-induced internal excitation of the drifting ions. The effects of ion speed distributions have been examined by measuring the rate constants of O^+ reactions in He and Ar buffer gases in a flow-drift tube. The rate constants are significantly different in the two buffer gases and are remarkably consistent with the Monte Carlo speed distributions calculated by Lin and Bardsley. The effects of internal excitation of molecular ions drifting at high E/N have been examined by comparing flow-drift tube and variable-temperature flowing-afterglow measurements of several reactions where such excitation apparently has a pronounced effect.

* Supported in part by Defense Nuclear Agency

** On leave from the Institut für Atomphysik, University of Innsbruck.

M-4 Kinetic Theory of Ion Transport and Ion-Molecule Reactions in Electric Fields of Arbitrary Strength.* E. A. MASON and LARRY A. VIEHLAND, Brown U.--A systematic moment method is described for solving the Boltzmann equation for ion motion in electric fields of arbitrary strength. Shrewd choice of basis functions can produce rapid convergence. Mobility data as a function of field strength can be interpreted as a variation with an effective temperature characterizing the mean kinetic energy in the center-of-mass frame, and can be analyzed to determine accurate ion-atom potentials. Similar treatments can also be used for ion diffusion and for ion-molecule rate coefficient data, but convergence behavior is more erratic if cross sections increase rapidly with increasing energy. Implications for experimental applications are discussed.

*Supported by the U.S. Army Research Office.

SESSION NA

8:30 AM - 10:15 AM, Friday, October 24

Ballroom East

NEGATIVE IONS; BREAKDOWN

Chairman: J.T. Park, University of Missouri-Rolla

NA-1 Photodetachment of CO_3^{-*}. S. P. Hong and S. B. Woo, Univ. of Del. and E. M. Helmy, Del. St. College - Electron-detecting-drift-tube-photodetachment technique was used to measure the absolute photodetachment cross section, and the solar photodetachment rate of CO_3^-. The cross section was measured with the use of 19 color filters. By fitting the data with a least-squares program, we found that:

$\sigma=[a_1+a_2\lambda'+a_3\lambda'^2+a_4\lambda'^3]H(\lambda_0-\lambda)$

λ_0= 459 nm (2.69 eV)

λ'= (λ-385) nm

a_1= $(1.21\pm0.26)\times10^{-19}$ cm^2

a_2= $(-3.61\pm1.64)\times10^{-21}$ cm^2/nm

a_3= $(1.62\pm0.17)\times10^{-22}$ cm^2/nm^2

a_4= $(2.00\pm0.31)\times10^{-24}$ cm^2/nm^3

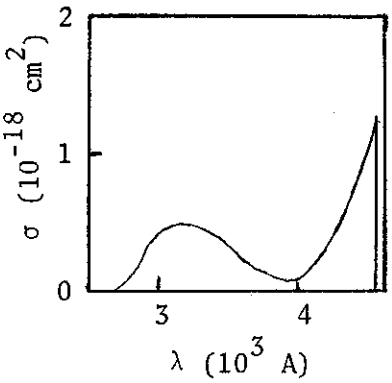

H is the Heaviside step function. The threshold energy was 2.69 ± 0.1 eV. The solar photodetachment rate was 0.022 ± 0.004. The CO_3^- was mass identified.

* Work supported in part by NASA.

NA-2 Formation and Decay of SF_6^{-*}. P. J. CHANTRY and C. L. CHEN, Westinghouse Research Laboratories.-- Attachment of low energy electrons to SF_6 at low pressure involves the reactions $e + SF_6 \rightleftharpoons SF_6^{-*} \rightarrow SF_5^- + F$. Published values of the SF_6^{-*} lifetime τ ranging from $\sim$ 10 μsec to $\sim$ 2 ms have been qualitatively reconciled[1] by invoking the expected, but previously undemonstrated dependence of τ on the electron energy. The present work demonstrates that the well known sharp zero energy peak in SF_6^- production is followed by a tail having an approximately exponential dependence on electron energy ε, i.e. $\exp(-\varepsilon/\varepsilon')$ where ε' decreases with increasing transit time through the mass-spectrometer. The results demonstrate that in this region of energy τ decreases with increasing electron energy, as expected. Increasing the temperature of the SF_6 leads to a decrease in ε', probably due to the increasing importance of the dissociative[2] decay channel.

[1]J.M.S. Henis and C.A. Mabie, J. Chem. Phys. 53, 2999 (1970).
[2]C.L. Chen and P.J. Chantry, Bull. Am. Phys. Soc. 15, 418 (1970).

NA-3 Low Energy (≲3 eV) Electron Attachment to C_2H_5Br in High Pressure Gases. R.E. GOANS and L.G. CHRISTOPHOROU, Oak Ridge National Laboratory--

Significant changes have been observed in both the magnitude and the energy dependence of the rate of attachment of slow (≲3 eV) electrons to bromoethane (C_2H_5Br) in dense N_2 and Ar gases with increasing density of these media from 500 to 25,000 Torr for N_2 and from 500 to 42,000 Torr for Ar. These results will be presented and discussed. The rate, R_L, of formation of $C_2H_5Br^{-*}$ at liquid N_2 (or Ar) density and the relative magnitudes of the dissociation and autoionization rates of $C_2H_5Br^{-*}$ have been determined as a function of mean electron energy, $\langle\epsilon\rangle$, from a model of the high pressure data. For $\langle\epsilon\rangle \ll 0.8$ eV (peak energy of the Br^- cross section) autoionization is the predominant channel of decay of $C_2H_5Br^{-*}$ while for $\langle\epsilon\rangle \gg 0.8$ eV the main decay channel is that of dissociation. At 0.8 eV $R_L = 1.5 \times 10^{-10} cm^3 sec^{-1}$. The lifetime of $C_2H_5Br^{-*}$ is estimated to be ≳13 picoseconds in the range $0.3 \leq \langle\epsilon\rangle \leq 1$ eV. The present results imply that the adiabatic electron affinity of C_2H_5Br is positive in spite of the fact that its vertical attachment energy is ~0.8 eV. (Research sponsored by the ERDA under contract with Union Carbide Corporation.)

NA-4 Temporary Negative Ions in Unsaturated Hydrocarbons P.D. BURROW, K.D. JORDAN, and J.A. MICHEJDA, Yale U. --
Temporary negative ion formation in ethylene and 1,3-butadiene has been studied using high[1] resolution, low energy electron transmission. Sharp structure in the total electron scattering cross section allows the adiabatic electron affinity to be determined leading to values of -1.55 ± 0.1 eV for ethylene and -0.62 ± 0.05 eV for 1,3-butadiene.[2] A series of dienes with the two ethylenic units separated by varying distances was also studied and the splitting between the two resonances used to establish the interaction between the double bonds. The information obtained on the unfilled orbitals of these hydrocarbons is complementary to that on the filled orbitals derived from photoelectron spectroscopy.

1. L. Sanche and G.J. Schulz, Phys. Rev. A 5, 1672 (1972).
2. P.D. Burrow and K.D. Jordan, submitted to Chem. Phys. Letters.

NA-5 Net Ionization Coefficient in SF_6. D. K. DAVIES, Westinghouse Research Labs.--Values of the net ionization coefficient λ_1 in SF_6 have been determined from spatial current growth measurements in uniform fields E over the range $3.4 \times 10^{-15} \leq E/N \leq 2.0 \times 10^{-14}$ V cm^2 for gas densities N in the range $3.5 \times 10^{16} \leq N \leq 8.8 \times 10^{17}$ cm^{-3}. Values of the ionization and effective attachment coefficients have also been determined over the range $3.4 \times 10^{-15} \leq E/N \leq 4.3 \times 10^{-15}$ V cm^2. Within experimental uncertainty, all the coefficients are found to be functions of E/N only. The limiting value of E/N, at which $\lambda_1 = 0$, is found to be 3.62×10^{-15} V cm^2. The present work extends the range of E/N of previous measurements by a factor of three. Good agreement with previous values of λ_1/N is found for the overlapping region of E/N.

NA-6 Measurement of Breakdown Potentials & Townsend Ionization Coefficients for the Penning Mixtures of Neon and Xenon. A.K. BHATTACHARYA, General Electric Company--

The Townsend primary (α), secondary (γ) coefficients and Paschen curves for nwon, xenon and their mixtures are reported. The primary coefficient was determined by measuring the variation in the luminous-flux in a self-sustained Townsend discharge between two parallel plate nickel electrodes spaced 21.5 mm apart. The values of the reduced primary coefficient, α/p, for Ne and Xe are about 10-20% lower than published values obtained by the classical method of Townsend. The α/p_o-values obtained for Ne agree with previous work using the same luminous-flux method. The ionization efficiency function η ($\eta = \alpha/E$, where E is the electric field) has a maximum value for Ne and 0.01% Xe. Also, the value of η for this gas mixture is larger than that for Ne + 0.1% Ar, especially at small values for E/p_o (1 to 10 V cm^{-1} torr^{-1}).

NA-7 Breakdown Measurements in Mercury-Argon Mixtures. H.L. Witting, General Electric Research and Development Center, Schenectady, N.Y. -- DC breakdown measurements were made in mercury-argon mixtures in cylindrical arc tubes. The mercury vapor pressure ranged from a few microns to 1 Atm, and the reduced argon pressure was 25 Torr. The breakdown voltage increased exponentially with the mercury reservoir temperature up to the point of complete mercury volatilization, and then decreased gradually. For a 7 cm arc gap, a maximum breakdown voltage of 6 kv was found at 350°C and 670 Torr. Current-voltage traces were recorded in the sub-mA range, covering the transition between a diffuse glow and a constricted arc. The effects of an auxiliary cathode discharge and of thermionic emission from a heated cathode were determined.

NA-8 Configurational Instability in Extended Plate-Wire Corona*. Yong Wook KIM, Lehigh U.-- When charged either positively or negatively, the wire of a wire-grounded plate corona exhibits, in the absence of corona current, small amplitude oscillations of broad frequency spectrum due to a number of noise contributions. Starting with the onset of corona current, the negatively charged wire undergoes a transition to large amplitude oscillations of the natural frequency of the given wire and its overtones, whereas no such transition is observed for the positively charged wire. We have first obtained the space charge and electric field strength distribution for a corona discharge in atmospheric air by numerical simulation. An equation of motion for the wire in this corona field is set up and its linearized solution obtained. Results show the onset of large amplitude oscillations for the negatively charged corona wire but not for the positive wire. In this treatment, the instability is seen to grow out of a phase shift originating from the difference in the hydrodynamic drag experienced by the oscillating wire and by a column of positive ions surrounding the wire.

*Work supported by Pennsylvania Power and Light Co.

SESSION NB

8:30 AM - 10:15 AM, Friday, October 24

Ballroom West

TRANSPORT PROPERTIES AND DISTRIBUTIONS

Chairman: G.L. Rogoff, Westinghouse

NB-1 Electron Distribution Function and Excitation Rates in N_2.* L.A. NEWMAN and T.A. DeTEMPLE, Univ. of Ill.--The need for accurate electronic excitation rates pertinent to gas discharge lasers has motivated electron distribution function calculations in molecular nitrogen. The calculation utilizes recently published and unpublished electron impact data to determine a new self-consistent set of vibrational and electronic cross sections by matching calculated transport data to experiment. Although the present set of electronic cross section is understandably different from those obtained in the earlier work of Engelhardt, Phelps and Risk, the newly calculated transport data (ν_u/N, ν_m/N, α_i/N are considered to be in good agreement with previously measured data[1]. The set of cross sections along with the calculated distribution function and vibrational and electronic excitation rates will be presented.

[1]A.G. Engelhardt, A.V. Phelps, and C.G. Risk, Phys. Rev., 135, 1566A (1964).

NB-2 Theory of Electron Drift Velocity Measurements in Parallel Plate Geometry.* J.H. WHEALTON, A.V. PHELPS and D.S. BURCH, JILA, U. of Colorado and NBS.--Experiments designed to measure electron drift velocities and diffusion coefficients are analyzed considering the effects on the arrival time spectra of electron ejection from an absorbing cathode, absorbing anode, circuit time constant and ionization. Diffusion theory shows that absorbing electrodes cause corrections to the drift velocity which are of the order of the energy relaxation distance divided by the drift tube length, β, for the cathode but are second order, $O(\beta^2)$, for the anode. We investigate the cathode effects more closely with a Monte Carlo calculation, which shows cathode corrections to vary with initial velocity and collisional energy losses. For a fast response external circuit and for injection normal to the cathode with a speed equal to the mean steady state value, the fractional increase in the apparent drift velocity caused by the cathode is 0.6 β, while the net increase is 1.6 β.

*Supported in part by Defense Advanced Research Projects Agency via ONR and ARO (D).

NB-3 The Effect of Absorbing Boundaries on the Distribution Function for Electrons in a Uniform Electric Field in a Gas. J. J. LOWKE, J. H. PARKER, JR., and C. A. HALL, Westinghouse Research Labs. The Boltzmann transport equation in f_o, the first term of a two term spherical harmonics expansion of the distribution function, has been solved for the case of a uniform steady stream of electrons being collected at an absorbing plane electrode due to the influence of a uniform electric field in a background gas. Steady state numerical solutions of f_o are obtained as a function of both energy and position for various power law dependencies of the momentum transfer cross-section on energy. Solutions of the electron density, n, as a function of position, differ significantly from the conventional solutions obtained by solving the transport equation in terms of drift and diffusion coefficients W and D, i.e. $\nabla\cdot(n\vec{W}-D\nabla n) = 0$. The drift and diffusion coefficients derived from the numerical solutions are functions of position and do not correspond with the diffusion coefficients derived previously for diffusion either transverse or parallel to the electric field. The derived average electron energy is enhanced by as much as 50% for positions where there is a large electron density gradient.

NB-4 Electron Boltzmann Transport Analysis of Potential Alkali Excimer and Dimer Laser Systems, L.A. SCHLIE & R.P. BENEDICT, Air Force Weapons Lab, Kirtland AFB, NM 87117. --- The Boltzmann Transport Equation including elastic, inelastic, ionization, electron-electron and electron-ion processes has been numerically solved for potential alkali excimer and dimer electrically excited laser discharges. These solutions indicate that for pure Na and Cs and Na-He and Cs-He mixtures, nearly 100% of the electron energy is transferred to the first electronic potential lasing state of the Cs and Na atoms in the E/N range from 10^{-16} to 10^{-15} $V\cdot cm^2$. For Na-Xe and Cs-Xe excimer mixtures having ratios of 1 Torr of the alkali and 10 Atm of xenon, over 90% of the electron energy is transferred to the first electronic state of the alkali atoms in the E/N range from 10^{-17} to 10^{-16} $V\cdot cm^2$. Due to the very large cross sections for the first electronic state of the alkalis, electron-electron interactions have negligible effect on the tail of the electron distribution even at partial ionizations (n_e/N) as high as 5%. Available cross sections, drift velocity, and characteristic energy data for the alkali will be discussed. These calculations will be generalized to all the alkali excimer and dimer potential laser systems.

NB-5 The Electron Energy Distribution Function in Electrically-Excited Molecular Gases, MANUEL GARCIA & GEORGE GIENKOWSKI, Princeton University --

The kinetic equation for the spherically symmetric part of the electron energy distribution function in the presence of an imposed electric field and dominant inelastic collisions is reformulated. The new form of the equation is suitable both for obtaining approximate solutions and for exact numerical computation via an iterative scheme. The formulation is particularly suitable in situations where vibrational excitation and de-excitation are both important. Some preliminary results for electron distributions and power input into vibration in CO gas are presented for several effective vibrational temperatures.

NB-6 The Mobility of Atomic Kr^+ and Xe^+ Ions in the $^2P_{3/2}$ and $^2P_{1/2}$ State in their Parent Gases. H. HELM, Australian National Univ. Australia--The influence of the spin state on the mobility of atomic ions in their parent gases krypton and xenon has been examined at room temperature using the Bradbury-Nielsen technique. In both cases the mobility of the ground state ions in the ($^2P_{3/2}$) state was found to be lower than that of the metastable ions in the $^2P_{1/2}$ state, the difference being 3.3% in krypton and 6% in xenon. This can be explained on the basis of the different potentials arising from the interaction of ground state and metastable state ions with their parent neutral atoms. A difference in reactivity was found for atomic ions in krypton depending on their spin state. The rate coefficient for the three-body conversion to Kr_2^+ was found to be higher for the ground state ion. No difference in reactivity was found for the different spin states in xenon indicating that the interaction of Xe^+ ($^2P_{1/2}$) + Xe gives rise to a stable configuration of Xe_2^+.

NB-7 Transport Properties of Positive & Negative Ions in CO_2. R.Y. PAI, H.W. ELLIS, I.R. GATLAND, and E.W. McDANIEL, Georgia Tech. --We have determined with a drift tube mass spectrometer the dominant species and transport coefficients of positive and negative ions formed by electron bombardment of CO_2. For positive ions the dominant species above 100 μ pressure are O_2^+ and its clusters $O_2^+ \cdot (CO_2)_n$. Since attachment is a two-body process, the ratios $[O_2^+ \cdot (CO_2)_{n+1}]/[O_2^+ \cdot CO_2)_n]$ increase with pressure and the average mobility decreases with pressure. Reaction rates of $O_2^+ + 2CO_2 \leftrightarrow O_2^+ \cdot CO_2 + CO_2$ can be inferred from our data. A typical value for the mobility K of the positive ion complexes if 1.25 cm^2/V-sec at 100 μ. For negative ions the dominant species is CO_3^- with K = 1.28 cm^2/V-sec. At our pressures (~ .1 -1 Torr), no clusters were seen but measurements at 1 atm indicate that $CO_4^- \cdot (CO_2)_n$ are the dominant complexes.

NB-8 Mobility Measurements of Aqueous Ions using a Wilson Cloud Chamber. LARRY E. STODDARD, PAUL C. YUE, and JAMES L. KASSNER, JR., Univ. of Missouri-Rolla - Interest in mobilities of atmospheric ions in environments saturated with water vapor has led to the development in this lab of a method of low-field mobility measurements of aqueous ion clusters using a Wilson cloud chamber. Two different ion sources have been developed for use in saturated environments, one using an electrical discharge and the other using alpha particle radiation. Ions from the discharge source have mobilities in the intermediate size range, several hundred water molecules. These ions are thought to be the result of a spraying process rather than of pure corona. Because the mobility of small ions plays an important role in determining the conductivity of clouds, we recently repeated our mobility studies using an ion source which utilizes the ions resulting from the energy loss of alpha particles. Three peaks in the mobility distribution indicating stable cluster sizes consisting of a few water molecules are observed. A modification of this ion source has also been developed to study the effects of ageing on the cluster distribution.

SESSION OA

10:30 AM - 12:15 PM, Friday, October 24

Ballroom East

ISOTOPE SEPARATION AND PHOTON INTERACTIONS

Chairman: D. Cartwright, Los Alamos

OA-1 Proposed Photo-Selective Isotope Separation by Dissociative Electron Attachment. C. L. CHEN and P. J. CHANTRY, Westinghouse Research Labs.--A number of examples are known where the reaction $e + XY \rightarrow X^- + Y$ is strongly enhanced for low energy electrons by heating XY, the effect being due to the presence of vibrationally excited XY. The application of this effect in a photo-selective isotope separation process, namely $h\nu + {}^1XY + {}^2XY \rightarrow {}^1XY^* + {}^2XY$, followed by ${}^1XY^* + e \rightarrow {}^1X^- + Y$, requires that the electrons compete effectively for ${}^1XY^*$ against excitation exchange reactions and radiative decay. Time dependent numerical solutions of the relevant rate equations determine the dependence of the performance parameters (separation factor, etc.) on the radiation intensity, the reaction time, and the densities of XY and [e]. In the favorable[1] example of SF_5^- production from SF_6 most of the required input data is available, permitting quantitative predictions of potential performance and identification of optimum operating conditions. In general the process has the notable merits of modest laser power requirements, and relative insensitivity to charge transfer mixing effects.

[1]C.L. Chen and P.J. Chantry, Bull. Am. Phys. Soc. 15, 418 (1970).

OA-2 Coherent Multiple Photon Excitation of Molecules* B.J. FELDMAN AND C.J. ELLIOTT. Los Alamos Scientific Laboratory--Pulsed laser driven dissociation and isotope separation have been reported for several polyatomic molecules. To understand the initial phase of this process, we have studied the interaction of an intense laser field with quantum mechanical N level anharmonic systems. The problem is treated by the diagonalization of the N x N Hamiltonian matrix. The rate of excitation of the system is studied as a function of laser frequency and intensity. In the limit $\mu E/\hbar$ > anharmonicity we obtain analytic solutions using orthogonal polynomials. Relaxation of selected energy levels and analogous classical systems are also studied. Implications of this work for multiple photon dissociation of polyatomic molecules are discussed along with models for the excitation process into higher lying dissociative and predissociative states.

*Work performed under the auspices of USERDA.

OA-3 Radial Cataphoresis of Selectively Ionized Isotopes
GERALD L. ROGOFF, Westinghouse Res. Labs.--Ambipolar diffusion can be an effective pumping mechanism for a selectively ionized isotopic species in a low-pressure gas mixture. If sufficient ion and electron densities are reached, ambipolar space-charge electric fields can lead to pumping of that species away from the ionization region. With the plasma bounded by a cylindrical wall at which recombination occurs, the ionization and subsequent radial cataphoresis can cause considerable depletion of the isotope near the axis and enrichment near the wall. The effectiveness of this process increases with the electron-to-ion characteristic-energy ratio (e.g., with applied electric fields) provided significant nonselective electron-impact ionization is avoided. A time-dependent computer model has been developed to describe the diffusion process. Included are effects of charge transfer, the only isotope exchange mechanism of concern after ionization. Calculations have been carried out for the case of atomic uranium of natural isotopic abundance in a tube with argon as a buffer. An external radiation source with a variable intensity profile is assumed to cause selective photoexcitation of ^{235}U leading to ionization. The results indicate significant radial pumping of ^{235}U with minor charge-transfer effects.

OA-4 Photoionization of $6^2P_{3/2}$ Cesium Atoms. E.H.A. GRANNEMAN, M.J. VAN DER WIEL, M. KLEWER and K.J. NYGAARD*, FOM-Institute for Atomic and Molecular Physics, Amsterdam, The Netherlands.--We have measured the relative cross section for photoionization of $Cs(6^2P_{3/2})$ atoms and found a shape proportional to λ^2 using 7 Argon ion laser lines in the range from 5017 to 4545 Å. The accuracy of the measurements is about $\pm$ 5%, as compared to $\pm$ 30% in the previous measurements of Nygaard et al.[1]. The Cesium atoms were excited by light from a pulsed GaAs laser, resulting in total count rates in excess of 10^4 sec^{-1}. The degree of polarization has been studied using circularly polarized light for excitation.

* Permanent address: Univ.of Missouri - Rolla, USA.

[1] K.J. Nygaard, R.E. Hebner Jr., J.D. Jones and R.J. Corbin, Phys.Rev. A (in press).

OA-5 The Importance of Hybrid Resonances in the Multiphoton Ionization of Cesium and Rubidium.* D. POPESCU, Inst. of Physics of Bucharest, Romania, I. POPESCU, U. of Bucharest, Romania, C.B. COLLINS, B.W. JOHNSON, S.M. CURRY, M.Y. MIRZA, M.A. TCHELEMALZADEH, J.A. ANDERSON, U. of Texas at Dallas--At most wavelengths the multiphoton ionization of alkalis can be viewed as a composite of the wings of transition resonances of purely atomic or molecular character. Recently the domain of multiphoton spectroscopy has been enlarged through the identification of hybrid resonances in which one-transition occurs to a dissociative state of the molecules and one between resulting atomic states. These hybrid resonances enlarge the multiphoton ionization probability and provide the experimental basis for ordering repulsive states of the molecules and correlating them with dissociation limits.

*Conducted as part of the U.S.-Romanian Co-operative program in Science and Technology between the U. of Texas at Dallas and the Institute of Physics and U. of Bucharest. Support was provided in part by NSF Grant GF443 and in part by the Romanian CSEN and CNST.

OA-6 Resonance Ionization Spectroscopy on He(2^1S).* G. S. HURST, M. G. PAYNE, M. H. NAYFEH,† J. P. JUDISH, C. H. CHEN,† E. B. WAGNER, and J. P. YOUNG, Oak Ridge Nat'l. Lab. -- We have developed a photoionization method for complete conversion of a quantum selected population to ionization, making possible sensitive and absolute measurement of the selected populations in a gas. Each photoionization involves the absorption of two photons (from a 1 J/pulse dye laser), one of which is resonant with an intermediate state. The absolute number of He(2^1S) states/ion pair following interaction of pulses of 2-MeV protons with He was measured. We have also demonstrated that quantum selected populations of He(2^1S) can be converted completely to ionization by single photon excitation to He(3^1P) followed by collision-induced associative ionization. For He pressures between 15 and 100 Torr, saturation of ionization was observed whenever a tunable dye laser produced more than 0.1 J/pulse.

*Research sponsored by the Energy Research and Development Adm. under contract with Union Carbide Corp.
†Postdoctoral research appointment through the Univ. of Kentucky supported by Los Alamos Scientific Laboratory.

OA-7 Diffuse Resonance Scattering of White Light by Sodium.* T. FUJIMOTO and A.V. PHELPS, JILA, U. of Colorado and NBS.--The spectral intensity of diffuse forward and back scattering of white light by sodium has been measured at wavelengths near the 589.0 and 589.6 nm resonance lines. The sodium density was varied from 3×10^{11} to 3×10^{15} cm^{-3} and the cell thickness was 4 mm. The measurements are made in a cell with plane parallel windows and are referenced to the light scattered by a $BaSO_4$ surface so as to allow comparison with theory.[1] Measured integrated absorption values are in good agreement with theory for sodium densities below 10^{12} cm^{-3} and above 7×10^{14} cm^{-3}. In the latter case asymmetry of the line is included. At intermediate densities the theory is less certain because of hyperfine components of the resonance lines. Measured integrated diffuse forward and back scattering intensities are compared with theory.

*Supported in part by Defense Advanced Research Projects Agency via ONR and ARO(D).

[1]A.V. Phelps and C.L. Chen (unpublished); D.G. Hummer and P. B. Kunasz, J. Quant. Spectrosc. Radiat. Trans. (in press).

OA-8 Vacuum Ultraviolet Absorption Spectra of Heteronuclear Diatomic Rare Gas Molecules. D. E. FREEMAN, K. YOSHINO, and Y. TANAKA, AFCRL, Bedford, Mass.--VUV absorption spectra of binary mixtures Xe/X (X = He, Ne, Ar, or Kr), originating from the ground electronic states of the van der Waals molecules XeX, have been photographed with a high resolution spectrograph in the 1080-1500 A region. Strong absorption bands occur near strong atomic lines, and we report now those observed near the first and second XeI resonance lines. These molecular spectral features extend mainly towards shorter wavelengths. In all cases except Xe/He near the first resonance line, discrete absorption bands are observed, and the extent of their formation increases with increasing molecular weight of XeX. The groups of bands of XeX at shortest wavelength near either resonance line are the most diffuse. XeKr exhibits sharper bands immediately to the short and long wavelength sides of the first and to the long wavelength side of the second resonance line, whereas XeAr exhibits such bands on both sides of only the second resonance line. The nature of the excited molecular states is relevant to possible laser action in rare gas mixtures.

SESSION OB

10:30 AM - 12:15 PM, Friday, October 24

Ballroom West

GLOW DISCHARGES

Chairman: R. Corbin, University of Missouri-Rolla

OB-1 TWO-DIMENSIONAL, TIME DEVELOPMENT OF PLASMA INSTABILITIES. W.H. LONG JR. and A. GARSCADDEN, AF Aero Propulsion Laboratory, WPAFB, Ohio---- The equations of a weakly ionized molecular gas in a uniform electric field are solved as a function of time and two spatial dimensions. Cylindrical symmetry is assumed about the field direction. The initial steady-state solution is perturbed by applying a localized ion density increase. The wavelike instabilities which develop are identified with those predicted previously from an analysis of the dispersion relation. In a plasma with only electrons and positive ions the waves are damped. In the presence of negative ions, the instability is absolute and propagates in the direction of the anode. There is also observed a damped oscillation, in the form of a wake, moving toward the cathode. The equation of heat conduction is included in the calculations, and it is shown how field and density fluctuations can develop into thermal instabilities on a longer time scale.

OB-2 Maintenance Electric Fields in a H_2-He dc Glow Discharge.* C.H. MULLER† and A.V. PHELPS, JILA, U. of Colorado and NBS.--Measurements have been made of E/N versus total pressure in a low current, cylindrically confined glow discharge in mixtures of 1 to 4% H_2 in He. The Boltzmann equation was solved using published cross sections[1] to obtain ionization rate coefficients. The ionization rate was balanced against ambipolar diffusion to predict E/N versus total pressure. The loss of electrons by ambipolar diffusion includes corrections for finite space charge sheaths,[2] the transition to free fall of the ions[3] and changes in ion identity. Good agreement between experiment and theory is obtained for total pressures of 5 to 300 torr in a 4 mm diameter tube. The range of E/N was 4×10^{-16} to 5×10^{-17} V-cm^2. Discharge currents varied from 40 to 100 μA.

*This paper was withdrawn prior to the 1974 GEC.

†Supported in part by NSF Grant No. MP572-05169-A02.

[1]A.G. Engelhardt and A.V. Phelps, Phys. Rev. 131, 2115 (1963); L.S. Frost and A.V. Phelps, Phys. Rev. 136, A1538 (1964).

[2]W.P. Allis and D.J. Rose, Phys. Rev. 93, 84 (1954); A.V. Phelps, Adv. in Chemistry 80, 18 (1969).

[3]S.A. Self and H.N. Ewald, Phys. Fluids 9, 2486 (1966).

OB-3 Calculation of the Cathode Region of a Glow Discharge.* G. FOURNIER, and D. PIGACHE, Office National d'Etudes et de Recherches Aérospatiales (ONERA).— The new Allis theory of the cathode fall† is developped in order to be solved numerically. Results are obtained for a gas model with one excitation level and one ionization level. The order of magnitude of the cathode fall is correct and the electric field is nearly linear with the distance. At the contrary of classical theory, the ionization coefficient increases with the distance from the cathode. The electron energy distribution at the entry of the negative glow is rather flat (between 0 and the cathode fall value). As a function of (current density/pressure squared), the cathode fall and the electric field at the cathode increase but the thickness of the dark space is nearly constant (for a constant secondary emission coefficient). The dark space properties do not depend on an auxiliary ionization source.

*Submitted by J. TAILLET
†W.P. Allis, Rev. Phys. Appl. 10, 97 (1975).

OB-4 Molecular radiation from a pure Hg constricted positive column, E. R. MOSBURG, NBS-A constricted positive column discharge of 30 to 400 mA in mercury vapor at temperatures of about 600K and densitites in the range 10^{18} to 6.4×10^{18} cm^{-3} (60 to 400 torr) has been studied in order to characterize the discharge and its relations to the measured molecular band emission and excimer densities. Three distinct temperatures are apparently involved; an electron temperature of 5000 to 8000 K, a neutral gas temperature of 650 to 700 K in the discharge column and an excimer vibrational temperature of 1200 to 1600 K. At 0.75 Pascals (100 torr) and for 30 mA the density of the $^3\Sigma_u$ excimer was estimated to be $\sim 3 \times 10^{9}$ cm^{-3} and the total excimer density to be $\sim 10^{12}$ cm^{-3} reinforcing the idea that an excimer storage level is present. The pressure dependence of this density will be discussed. There is evidence, based on Abel inversion of spacial projected light intensity profiles, that the $^3\Sigma_u$ is destroyed by electrons in the conducting column. Optical absorption measurements made in order to establish the density of the $^3P_0$, $^3P_1$, $^3P_2$, and $^1P_1$ levels will also be discussed.

OB-5 **Measurements of the Ambipolar Field in the Positive Column of Neon Discharges**, R.M.M. SMITS, M. PRINS, & J.A. V.D. HEIDE, Univ. of Technology, Eindhoven, Netherlands--
Measurements of the ambipolar field in the positive column of neondischarges with pressures of 100 and 200 torr and currents between 5 and 100 mA are presented. For these measurements a diagnostic method which involves the use of radioactive tracers was used. The experimental results are compared with predictions derived from a theoretical model of the positive column. For 100 torr and currents of 15, 40 and 80mA measured values of the radial derivative of the ambipolar field strength at the discharge axis are resp. 2.4, 2.8 and 3.4 V/cm^2 and computed values resp. 2.4, 2.9, and 3.5 V/cm^2. For 200 torr and currents of 5.15,40 and 80mA the experimental values are resp. 1.5, 3.5, 4.6 and 5.8 V/cm^2 and the theoretical values 2.2, 2.8, 3.8 and 5.6 V/cm^2.
At increasing distance from the discharge axis for the higher currents a maximum and then a minimum is found in the ambipolar field-strength.

OB-6 **Theory of Hollow Cathode Arc (HCA) in Argon**. J.L. DELCROIX, C.M. FERREIRA. Lab. Phys. Plasmas - Univ. Paris-SUD--
The theory of the HCA in Argon has been developed and the efficiency of this arc as a source of metastables discussed. The main parameters of the discharge are those of the plasma column inside the cathode: gas flow Q($\sim$1cm^3 s.t.p.), neutral density multiplied by radius n_0R($\sim 10^{16}$ cm^{-2}), neutral temperature T_0 (2000C) electron density n_e ($\sim 10^{13}$cm^{-3}) and temperature T_e (1-3 eV) metastable density n_M ($\sim 10^{12}$ cm^{-3}), cathode sheath potential U_0 (10-40 V) and current $i=i_{thermionic}(1+\alpha)$ ($\sim$10A) where α= 1-3 is the gaseous multiplication coefficient. Primary electrons are injected into the gas with the energy U_0 gained in the sheath. Analysis of their energy decay(1) give a relation between U_0 and α.Balance equations for n_M and T_e are then written and discussed(2)showing that n_M/n_0 is strongly depending on U_0 and better for low values of T_e; finally the energy balance of the cathode wall leads to relation between i and U_0 and by an iteration give a test of the self-consistency of the theory.(3)
(1) (2) C.M.FERREIRA,J.L.DELCROIX-J.de Phys.(à paraître)
(3) C.M. FERREIRA-Thèse de Doctorat ORSAY-Janvier 1976

OB-7 Decay of Na-resonance radiation in a Na-Ne afterglow*. M.J.C. VAN GEMERT and E.A. BINK**. Philips Research Labs., Eindhoven, Netherlands. -- The decay of Na-resonance radiation, in a Na-Ne afterglow (R=1cm, P_{Ne}=5.5 and 10 Torr), is measured as a function of current I, at wall temperatures between 230 and 260°C, corresponding to a Na-density between 1.1×10^{19} and $4.6\times10^{19}m^{-3}$. For $2\mu s \leq t \leq 6\mu s$ the decay is exponential with time constant τ_L. At low currents τ_L decreases with increasing I, reaching a sharp minimum at a certain critical value I_C. For $I > I_C$, τ_L increases again[1]. The value of τ_L at $I=I_C$ is remarkably independent of n_{Na}: τ_L=1.29 μs for $n_{Na}=1.1\times10^{19}m^{-3}$ and τ_L=1.36μs for $n_{Na}=4.6\times10^{19}m^{-3}$ (P_{Ne}=5.5 Torr). These values are in good agreement with those from model calculations[2]: τ_L=1.40μs and 1.48μs, respectively.

* Submitted by R. Bleekrode.
** Trainee from Delft University of Technology.

1. M.J.C. van Gemert, J.Appl.Phys., Nov. (1975).
2. H. van Tongeren, Philips Res.Repts. Suppl. No. 3, (1975) sec. 5.6.

Index to Abstracts

28th ANNUAL GASEOUS ELECTRONICS CONFERENCE
LIST OF PARTICIPANTS

Adawi, I.H.	UMR
Akerman, Alfred	University of Illinois
Albritton, Daniel L.	NOAA Research Labs
Aldag, John E.	UMR
Allis, William P.	MIT
Anderson, Jay H.	University of Illinois
Anderson, Richard	University of Arkansas
Anderson, Richard A.	UMR
Anicich, Vincent G.	Jet Propulsion Laboratory
Bailey, Thomas L.	University of Florida
Baltog, Ioan G.	University of Texas at Dallas
Bardsley, J. Norman	University of Pittsburgh
Barreto, Ernesto	SUNY-Albany
Beaty, Earl C.	JILA
Benedict, Rettig P.	AFWL
Benenson, David M.	SUNY-Buffalo
Bergman, Rolf S.	General Electric
Bhasin, Kul	UMR
Bhattacharya, Ashok K.	General Electric
Bhattacharya, Dilip	Institut de Recherche de l'Hydro-Quebec
Biondi, Manfred A.	University of Pittsburgh
Binns, W. Robert	McDonnell Douglas Research Laboratories
Bleekrode, Richard	Philips Research Laboratories
Bohn, W.L.	DFVLR Institut for Plasmadynamics
Boness, Michael J.	Avco Everett Research Lab
Bonifield, Thomas D.	Rice University
Brown, H.A.	UMR
Bryan, David A.	UMR

Bullis, Robert H.	United Technologies Research Center
Burnham, Ralph L.	Science Applications Inc.
Burrow, Paul D.	Yale University
Byron, Stanley	Mathematical Sciences Northwest
Callary, Paul R.	UMR
Carnahan, Byron L.	University of Pittsburgh
Cartwright, David C.	Los Alamos Scientific Lab
Champagne, Louis F.	NRL
Chang, Edward S.	University of Massachusetts
Chanin, Lorne M.	University of Minnesota
Chantry, Peter J.	Westinghouse Research Labs
Chen, C.L.	Westinghouse Research Labs
Chen, Chung-Hsuan	Oak Ridge National Laboratory
Chen, Hsing-Cheng	JILA
Cherrington, Blake E.	University of Illinois
Chubb, Donald L.	NASA Lewis Research Center
Chung, Sunggi	University of Wisconsin
Chutjian, Ara	Jet Propulsion Laboratory
Cohen, Ira M.	University of Pennsylvania
Crompton, Robert W.	Australian National University
Collins, Carl B.	University of Texas at Dallas
Collins, George J.	Colorado State University
Cook, James William	Square D Company
Cooper, Gary W.	University of Illinois
Corbin, Robert	UMR
Crane, John K.	University of Illinois
Dardis, John G.	Office of Naval Research
Davies, D. Kenneth	Westinghouse Research Labs
DeJoseph, Charles A. Jr.	Universal Energy Systems

Delcroix, Jean-Loup	Universite Paris-Sud
Deloche, Robert	Commissariat a L'Energie Atomique
DeTemple, Thomas A.	University of Illinois
Denes, Louis J.	Westinghouse Research Labs
deVries, Cyril P.	University of Minnesota
DeYoung, Russell J.	NASA
Dimoff, Kenneth	INRS-Energie, Quebec
Dolan, Tom	UMR
Douglas-Hamilton, D.H.	Avco Everett Research Labs
Drop, Peter C.	Philips Research Labs
Eckhardt, Gisela	Hughes Research Labs
Eddy, Thomas L.	West Virginia Institute of Technology
Eden, James G.	University of Illinois
Elliott, C. James	Los Alamos Research Lab
Farrall, George A.	G.E. R&D Center
Feeney, Robert K.	Georgia Institute of Technology
Fehsenfeld, Fred C.	NOAA Research Labs
Fiamengo, Nicholas A.	Aerospace Corporation
Fischer, Ernst H.	Philips Forschungslabor Aachen
Fitzsimmons, William A.	University of Wisconsin
Flannery, Ray	Georgia Institute of Technology
Fournier, Gerard F.	ONERA
Franklin, Richard D.	Air Force Weapons Lab
Freeman, Daryl E.	Air Force Cambridge Res. Labs
Frommhold Lothar	University of Texas-Austin
Fujimoto, Takashi	JILA
Gannon, Richard E.	Avco Everett Research Lab
Garrett, W.R.	Oak Ridge National Lab
Garscadden, Alan	AF Aero Propulsion Lab

Gentry, Alan	AF Aero Propulsion
George, Jerome M.	UMR
Gerardo, James B.	Sandia Labs
Gerson, Robert	UMR
Gleason, Robert E.	Rice University
Glickstein, Stanley S.	Westinghouse
Godard, Bruno M.	CGE Laboratory de Marcoussis
Graham, Walter J.	Naval Surface Weapons Center
Greene, Arthur E.	Los Alamos Scientific Laboratory
Harris, L.P.	General Electric Co.
Harwell, Roger B.	USAF Weapons Lab.
Hasker, Jan	Philips Research Labs
Haugsjaa, Paul O.	General Telephone Electronics Lab.
Hays, Gerald N.	Sandia Labs
Heberlein, Joachim V.R.	University of Minnesota
Hess, LaVerne D.	Hughes Research Labs
Hill, Alan E.	Air Force Weapons Lab
Hill, Robert M.	Stanford Research Institute
Hirshfield, Jay L.	Yale University
Hoff, Paul W.	U.S. ERDA
Hong, Siu-Ping	JILA
Huang, Chou-Mou	University of Pittsburgh
Hugel, Helmut E.	DFVLR-Inst. for Plasmadynamics
Hughes, William M.	LASL
Hurst, George S.	Oak Ridge National Labs
Ingold,John H.	General Electric
Jacob, Jonah H.	Avco Everett Research Lab
Johnson, A. Wayne	Sandia Labs

Johnson, Peter D.	General Electric
Johnsen, Rainer	University of Pittsburgh
Jones, Walter W.	Naval Research Laboratory
Kassner, James L., Jr.	UMR
Kazek, Gregory J.	General Electric
Keefe, William M.	GTE Sylvania
Keto, John W.	University of Texas-Austin
Kline, Laurence E.	Westinghouse Research Labs
Kramer, Gerry M.	GTE Laboratories
Ladish, Joseph S.	Los Alamos Scientific Lab
Lane, Neal F.	Rice University
Lake, Max L.	Universal Energy Systems
Lam, Sau H.	Princeton University
Lancaster, Beaufort	UMR
Land, James	JILA
Lawton, Stanley A.	JILA
Leland, W.T.	Los Alamos Scientific Lab
Leslie, Scott G.	University of Illinois
Liebermann, Richard	Westinghouse
Litke, John D.	Johns Hopkins University
Loeb, Sunard B.	University of California-Berkeley
Long, William H. Jr.,	Aero Propulsion Laboratory
Lorents, Donald C.	Stanford Research Institute
Lowke, John J.	Westinghouse Research Labs
Lund, Louis H.	UMR

MacRae, Donald R.	Bethlehem Steel Corporation
Madson, James M.	McDonnell Douglas Corporation
Mann, Michael	Northrop R&D Center
Mahadevan, P.	Aerospace Corporation
Mangano, Joseph A.	Avco-Everett Research Labs
Mason, Edward A.	Brown University
Matzen, M. Keith	Sandia Laboratories
Manuccia, T.J.	NRL
McArthur, David A.	Sandia Laboratories
McCusker, Michael V.	SRI
McFarland, Robert H.	UMR
McLaughlin, Robert W.	University of Pittsburgh
McNeil, John R.	Colorado State University
Mickish, Roger A.	AFWL
Miles, Richard B.	Princeton University
Miller, Clifford H.	JILA
Moeny, William M.	Kirtland AFB
Mosburg, Earl R.	National Bureau of Standards
Mukherjee, Deb	Stanford Research Institute
Muschlitz, E.E.	University of Florida
Nayfeh, Munir H.	Oak Ridge National Laboratory
Newman, Leon A.	University of Illinois
Nighan, William L.	United Technologies Research Center
Novak, Jaroslav P.	Hydro-Quebec Institute of Research
Nygaard, Kaare J.	UMR
Olson, Robert A.	Systems Research Labs
Oskam, Henrik	University of Minnesota
Pai, Robert Y.	Georgia Institute of Technology
Palmer, Kent F.	University of Kentucky

Park, John T.	UMR
Parks, W.F.	UMR
Partlow, William D.	Westinghouse Research
Payne, Marvin	Oak Ridge National Lab.
Peacher, Jerry L.	UMR
Pendleton, William R. Jr.	Utah State University
Persson, Karl-Birger	National Bureau of Standards
Pfender, Emil	University of Minnesota
Phelps, Arthur V.	JILA
Phelps, James O.	University of Wisconsin
Plummer, Michael J.	U.S. Naval Surface Weapons Center
Powell, Howard T.	Lawrence Livermore Lab
Prince, John F.	Aero Propulsion Lab
Prokopenko, Susan M.L.	University of Florida
Rambow, Frederick H.K.	UMR
Read, Frank	University of Manchester, England
Reagan, Roger L.	UMR
Ricard, Andre	Physique Plasmas
Rice, James K.	Sandia Laboratories
Rich, Joseph	General Electric
Rockwood, Stephen	LASL
Rogoff, Gerald L.	Westinghouse Research Labs
Roiseland, Donald S.	Wartburg College
Rothe, Dietmar E.	Lumonics Research Limited
Rumble, John	JILA
Sagmuller, Joseph R.	Battelle Memorial Institute
Sahni, Omesh	IBM Thomas J. Watson Research Center
Saporoschenko, M.	Southern Illinois University
Sargeant, Jim	National Research Council

Schearer, Laird D.	UMR
Schlie, LaVerne A.	Kirtland AFB
Schnable, Edwin M.	Western Electric
Schuebel, W.K.	Wright-Patterson AFB
Schulz, George J.	Yale University
Searles, Stuart	Naval Research Laboratory
Sexton, Michael C.	University College, Cork Ireland
Shepherd, William B.	Boeing Aerospace
Sides, Gary D.	Wright State University
Sipler, Dwight	University of Pittsburgh
Skipper David J.	UMR
Smith, Felix T.	Stanford Research Institute
Smith, Stephen	NSF, Washington
Snow, W.R.	UMR
Springer, Robert H.	General Electric
St. John, Robert M.	University of Oklahoma
Stevens, Walter J.	National Bureau of Standards
Stoddard, Larry E.	UMR
Suhre, Dennis R.	University of Illinois
Taylor, Lyle H.	Westinghouse Electric
Tchellehmalzaden, Mohammadali	University of Texas at Dallas
Thieneman, Michael	University of Kentucky
Theiss, Paul E.	University of Illinois
Tisone, Gary C.	Sandia Laboratories
Tracy, Clarence J.	University of Minnesota
Van Brunt, Richard	JILA
van der Heide, J.A.	Univ. of Technology, Eindhoven
Varney, Robert N.	U.S. Army Ballistic Research Labs
Verdeyen, Joseph T.	University of Illinois
Viehland, Larry A.	Brown University

Walker, Keith G.	Bethany Nazarene College
Waller, Robert A.	University of Texas at Dallas
Walters, G. King	Rice University
Wang, S.K.	Xerox Corporation
Ward, Carolyn	UMR
Watson, James	University of Arkansas
Waymouth, John F.	GTE Sylvania
Weisbach, Michael	Boeing
Weissler, Gerhard L.	University of Southern California
Wells, William E.	University of Illinois
Whealton, John	JILA
Winans, J. Gibson	SUNY - Buffalo
Witting, Harald L.	General Electric
Wong, Shek-Fu	Yale University
Woodworth, Joseph R.	Sandia Laboratories
Wu, Yen Chang	UMR
Yoder, Marcel J.	Avco Everett Research Lab.
Zenor, Hughes M.	UMR
Zollweg, Robert J.	Westinghouse Research Labs